Solid Earth

Orogenic lithosphere and slabs in the greater Alpine area – interpretations based on teleseismic P-wave tomography

Mark R. Handy[1]**, Stefan M. Schmid**[2]**, Marcel Paffrath**[3]**, Wolfgang Friederich**[3]**, and the AlpArray Working Group** ✚

[1]Institut für Geologische Wissenschaften, Freie Universität Berlin, Malteserstr. 74–100, 12249 Berlin, Germany
[2]Institut für Geophysik, ETH-Zürich, Sonneggstr. 5, 8092 Zurich `CE1`, Switzerland
[3]Institut für Geologie, Mineralogie, Geophysik, Ruhr-Universität Bochum, 44780 Bochum, Germany
✚For further information regarding the team, please visit the link which appears at the end of the paper.

Correspondence: Mark R. Handy (mark.handy@fu-berlin.de)

Abstract. Based on recent results of AlpArray, we propose a new model of Alpine collision that involves subduction and detachment of thick (~ 180 km) European lithosphere. Our approach combines teleseismic P-wave tomography and existing local earthquake tomography (LET), allowing us to image the Alpine slabs and their connections with the overlying orogenic lithosphere at an unprecedented resolution. The images call into question the conventional notion that downward-moving lithosphere and slabs comprise only seismically fast lithosphere. We propose that the European lithosphere is heterogeneous, locally containing layered positive and negative V_p anomalies of up to 5 %–6 %. We attribute this layered heterogeneity to seismic anisotropy and/or compositional differences inherited from the Variscan and pre-Variscan orogenic cycles rather than to thermal anomalies. The lithosphere–asthenosphere boundary (LAB) of the European Plate therefore lies below the conventionally defined seismological LAB. In contrast, the lithosphere of the Adriatic Plate is thinner and has a lower boundary approximately at the base of strong positive V_p anomalies at 100–120 km.

Horizontal and vertical tomographic slices reveal that beneath the central and western Alps, the European slab dips steeply to the south and southeast and is only locally still attached to the Alpine lithosphere. However, in the eastern Alps and Carpathians, this slab is completely detached from the orogenic crust and dips steeply to the north to northeast. This along-strike change in attachment coincides with an abrupt decrease in Moho depth below the Tauern Window, the Moho being underlain by a pronounced negative V_p anomaly that reaches eastward into the Pannonian Basin

area. This negative V_p anomaly is interpreted as representing hot upwelling asthenosphere that heated the overlying crust, allowing it to accommodate Neogene orogen-parallel lateral extrusion and thinning of the ALCAPA tectonic unit (upper plate crustal edifice of Alps and Carpathians) to the east. A European origin of the northward-dipping, detached slab segment beneath the eastern Alps is likely since its down-dip length matches estimated Tertiary shortening in the eastern Alps accommodated by originally south-dipping subduction of European lithosphere.

A slab anomaly beneath the Dinarides is of Adriatic origin and dips to the northeast. There is no evidence that this slab dips beneath the Alps. The slab anomaly beneath the Northern Apennines, also of Adriatic origin, hangs subvertically and is detached from the Apenninic orogenic crust and foreland. Except for its northernmost segment where it locally overlies the southern end of the European slab of the Alps, this slab is clearly separated from the latter by a broad zone of low V_p velocities located south of the Alpine slab beneath the Po Basin. Considered as a whole, the slabs of the Alpine chain are interpreted as highly attenuated, largely detached sheets of continental margin and Alpine Tethyan oceanic lithosphere that locally reach down to a slab graveyard in the mantle transition zone (MTZ).

1 Introduction

The prevailing paradigm of mountain building in the greater Alpine area (Fig. 1) involves subduction of European continental lithosphere that is some 100–120 km thick beneath
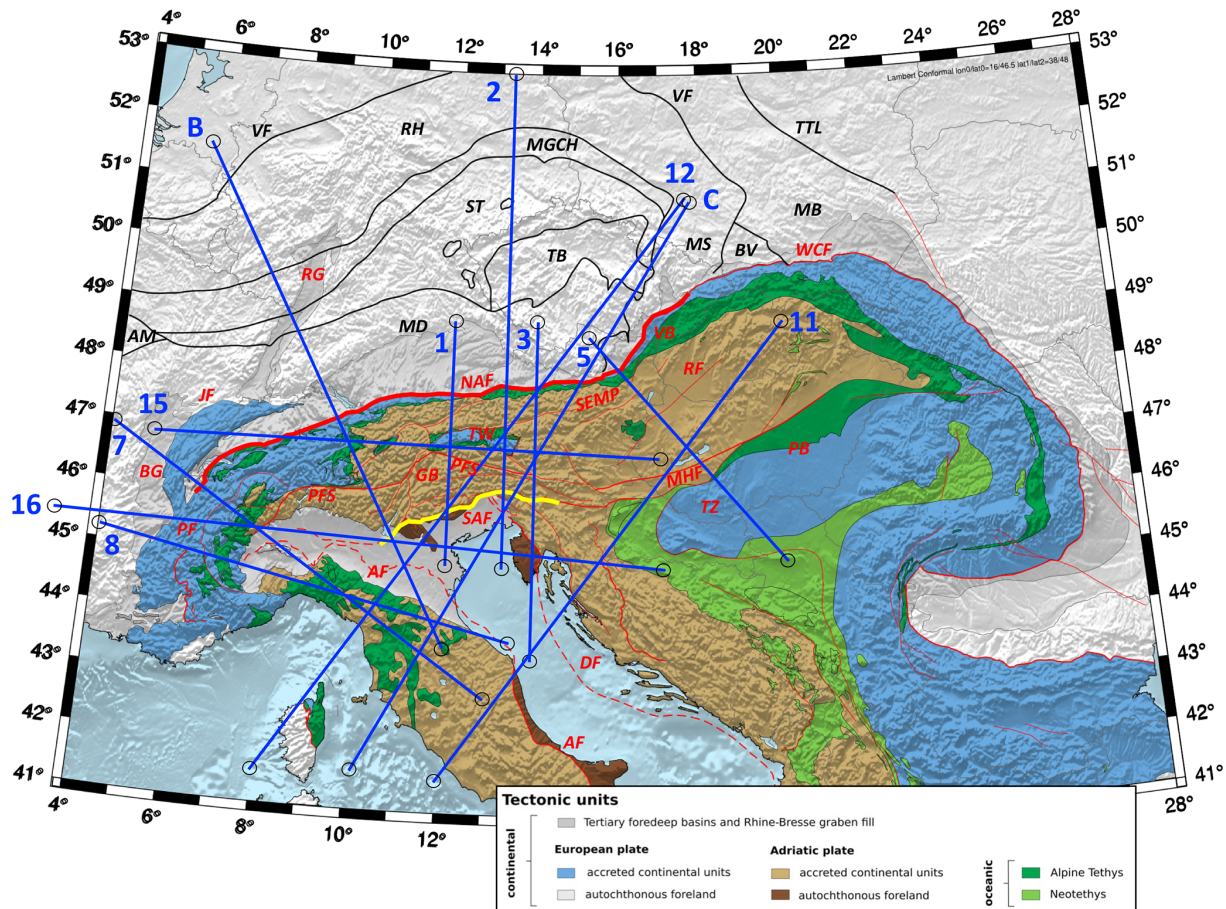
Figure 1. Tectonic map of the Alpine chain and its foreland, including Variscan units. Thin red lines – main Tertiary tectonic faults after Schmid et al. (2004) and (2008); thin black lines – tectonic lineaments separating Variscan tectonometamorphic domains after Franke (2017, 2000), Mazur et al. (2020) and Schulmann et al. (2014). Blue lines are traces of vertical tomographic profiles in Figs. 3–7. The numbers of the traces are in accordance with their appearance in Appendix A. Thick red line along the NAF marks the Oligo-Miocene plate boundary in the Alps; yellow line along the SAF marks the presently active plate boundary in the Alps; green units are the Adria–Europe suture marking the Late Cretaceous to late-Eocene plate boundary. Alpine faults and related structures: NAF – Northern Alpine Front; SAF – Southern Alpine Front; PFS – Periadriatic Fault System; GB – Giudicarie Belt; JF – Jura Front; PF – Penninic Front; RG – Rhein Graben; BG – Bresse Graben; TW – Tauern Window; SEMP – Salzach–Ennstal–Mariazell–Puch Fault; MHF – Mid-Hungarian Fault Zone; VB – Vienna Basin; PB – Pannonian Basin; RF – Raba Fault; WCF – Western Carpathian Front; DF – Dinaric Front: Variscan tectonic domains and faults: VF – Variscan orogenic front; RH – Rheno-Hercynian; MGCH – Mid-German Crystalline High; ST – Saxo-Thuringian; MD – Moldanubian; TB – Teplá–Barrandian; AM – Armorican Massif; BV – Brunovistulian; MB – Malopolska Block; MS – Moravo-Silesian. Other faults: TTL – Teysseyre–Thornquist Line.

the upper Adriatic Plate, lithosphere thickness being based largely on seismological criteria (Jones et al., 2010; Geissler et al., 2010; Kissling et al., 2006). We refer to this as the *standard lithosphere model* of continental subduction to distinguish it from a new model here involving the subduction and partial delamination of much thicker, compositionally heterogeneous European mantle. We base this model on recent P-wave images of the AlpArray seismological campaign (Paffrath et al., 2021b) presented below.

We use the terms *plate* and *slab* in a strictly structural–kinematic sense to refer to bodies of compositionally heterogeneous mantle and crust that have moved coherently with respect to markers in both the mantle and at the surface. As pointed out by Artemieva (2011), different geophysical techniques have given rise to a multitude of definitions of the lithosphere based on seismic, thermal, electrical, rheological and petrological properties. Our definition therefore differs from strictly seismological definitions, which treat plates as seismically fast mantle lithosphere (e.g. Piromallo and Morelli, 2003; Wortel and Spakman, 2000). Implicit in the structural–kinematic definition of lithosphere we use is that the base of the lithosphere is a shear zone that accommodates the relative motion of plates.

As in other orogenic belts, the standard model of lithospheric subduction in the Alps was initially supported by teleseismic body-wave studies showing fast seismic velocity anomalies dipping beneath the Alpine–Mediterranean mountain belts (Wortel and Spakman, 2000). They are often inclined in the same direction as the dipping Mohos that define the base of the orogenic crust (Waldhauser et al., 2002; Lippitsch et al., 2003; Spada et al., 2013). These seismically fast domains are inferred to reflect negative temperature anomalies that mark descending slabs of cold subcontinental lithospheric mantle, whereas positive anomalies at the base of, and surrounding, these seismically fast domains are often interpreted as warm asthenospheric mantle (e.g. Spakman and Wortel, 2004). In the Alps, the base of the subducting European Plate has thus been taken to be the boundary between seismically fast and slow domains (respectively, blue and red domains in most tomographic slices), whereas its top is the interface with the upper Adriatic Plate. Seismological studies in the western Alps have shown that this interface includes subducted crust down to depths of > 90 km (Lippitsch et al., 2003; Zhao et al., 2015, 2016), corroborating geological evidence of deeply subducted and exhumed fragments of oceanic and continental crust (e.g. Chopin, 1984; Schertl et al., 1991) and mantle (Brenker and Brey, 1997) preserved in the Alps (Agard and Handy, 2021).

When assessing the geometry of subduction and plate boundaries in the Alps, it is important to distinguish the Late Cretaceous–Paleogene Adria–Europe subduction plate boundary represented by the Tethyan ophiolite belt along the Alps (Fig. 1) from the Oligo-Miocene collisional boundary exposed along the Northern Alpine Front (labelled NAF in Fig. 1). Both of these boundaries differ from the Pliocene-to-active plate boundary along the Southern Alpine Front (SAF in Fig. 1). In the analysis below, these differently aged boundaries provide important kinematic and time constraints for the tectonic interpretation of mantle anomalies. None of these geological boundaries coincide at the surface, nor are they expected to merge at depth given that the Alps have experienced changes in the amount and direction of shortening with time (Schmid et al., 2004; Handy et al., 2010). This is especially true of the eastern part of the Alps, where Paleogene N–S shortening and subduction has given way to Mio-Pliocene eastward lateral extrusion of orogenic crust and possibly upper mantle (e.g. Ratschbacher et al., 1991) that is still ongoing during continued Adria–Europe N–S convergence (e.g. Grenerzcy et al., 2005; Serpelloni et al., 2016).

Controversy on Alpine subduction has arisen because the SE dip of the Alpine slab anomaly in the central and western Alps (Lippitsch et al., 2003; Zhao et al., 2015; Lyu et al., 2017) indicating "classical" SE-directed subduction of the European slab (e.g. Argand, 1924; Pfiffner et al., 1997; Schmid et al., 1996) contrasts with a dip to the northeast of a positive V_p slab anomaly in the eastern part of the chain, i.e. east of 12–13° E in Fig. 1 (Lippitsch et al., 2003; Mitterbauer et al., 2011; Karousová et al., 2013, Zhao et al.,

2016). This NE dip is inconsistent with SE-directed Alpine subduction inferred from the uniformly S dip and N- to NW-directed shear sense indicators of sutured oceanic lithosphere and crustal nappes all along the Alps (e.g. Schmid et al., 2004), including the eastern Alps (e.g. Handy et al., 2010, and references therein). The plate tectonic affinity of this part of the slab beneath the eastern Alps therefore remains unclear and debated. Proponents of a European origin propose the existence of a very steeply NE-dipping overturned to subvertically oriented slab that detached from the crust east of the Tauern Window (Mitterbauer et al., 2011; Rosenberg et al., 2018). Proponents of an Adriatic origin of this slab based their interpretation on the tomographic images of Lippitsch et al. (2013; their Fig. 13c) that depict a moderately NE-dipping slab still attached to the still undeformed parts of the Adriatic Plate. They therefore proposed a late-stage reversal of subduction polarity (Schmid et al., 2004; Kissling et al., 2006; Handy et al., 2015). A recent review by Kästle et al. (2020) that also takes surface wave tomography into consideration considers the possibility that this slab has a combined European–Adriatic origin, as discussed in Handy et al. (2015).

In this paper, we interpret vertical and horizontal tomographic slices of the Alps generated by integrating crustal and mantle tomographic P-wave models gleaned from the AlpArray seismological network (Hetényi et al., 2018). This new method, described in the next section and in detail in Paffrath et al. (2021b), employs teleseismic tomography and integrates the crustal and uppermost mantle models of Diehl et al. (2009) and Tesauro et al. (2008) as a priori information into the teleseismic inversion, weighted according to its reliability. This allows us to image the Alpine slabs and their potential connections with the orogenic edifice as well as the foreland and hinterland lithospheres at an unprecedented resolution. The images presented in Sects. 3 and 4 call into question the conventional notion based on seismological criteria that slabs comprise only seismically fast mantle lithosphere that is some 100–120 km thick. Instead, they suggest that the down-going European Plate in the Alps is much thicker and contains positive and negative seismic anomalies inherited from pre-Alpine (Variscan) events that, given their age, are likely to be of structural and compositional rather than thermal nature. In Sect. 5, we showcase evidence of large-scale delamination of the slabs in the Alps and Northern Apennines, with slabs that have been partly to entirely detached from their orogenic edifices. The discussion in Sect. 6 revisits the debate on subduction polarity in light of the new data and touches on some implications of widespread delamination and slab detachment for crustal seismicity and foreland basin evolution. We conclude with a conceptual 3D visualization of mantle structure beneath the Alps and Apennines that serves as a vehicle for assessing the interaction of slabs and asthenosphere at depths down to the mantle transition zone (MTZ).

2   Methodology

The images of velocity anomalies in this paper are derived from a 3D model of P-wave velocity in the crust and mantle below the greater Alpine region (Paffrath et al., 2021b). This is obtained by tomographic inversion of teleseismic P-wave travel-time residuals measured on records of the AlpArray Seismic Network (Paffrath et al., 2021a). Travel-time residual is the difference between the observed and a theoretical travel time calculated for a standard earth model. Calculation of the travel-time residuals and the inversion procedure are described here in turn, as outlined in Paffrath et al. (2021b, their chap. 2 and Appendix A1).

The travel-time database comprises 162 366 onsets of 331 teleseismic earthquakes of magnitude 5.5 or higher at epicentral distances between 35 and 135° occurring between January 2015 and July 2019. Paffrath et al. (2021b) subtracted the array average from these residuals on an event-to-event basis. This procedure avoids errors in earthquake origin time and reduces influences of heterogeneities in earth structure outside the inversion domain (see Paffrath et al., 2021a, on obtaining highly accurate travel-time residuals suitable for teleseismic inversion).

Inversion of the travel-time residuals to obtain the P-wave velocity perturbations in the depth slices and profiles of V_p anomalies below is a complex process. The aim of inversion is to find a model that reduces the misfit between the observations and predictions of travel times to a certain threshold value. Iteration of the inversion ends if either the observations fit within their uncertainties or if the misfit reduction stagnates when executing further iterations.

Because teleseismic waves propagate subvertically through the crust, the resolution of strongly heterogeneous crust is poor. Correcting for heterogeneities requires a velocity model of the crust, termed an a priori model (e.g. Kissling, 1993), which is based on independent data, e.g. reflection and refraction seismics, receiver functions and local earthquake tomography. The standard correction method involves computing travel-time residuals for the crustal model on the assumption of idealized wave fronts and then subtracting these residuals from the observed residuals. This oversimplifies the true ray paths, which are refracted in the crust and underlying mantle depending on vertical and azimuthal incidence.

The novel approach of Paffrath et al. (2012b) entails creating a starting model for inversion iteration by superposing a 1D standard earth model (here taken to be model AK135 of Kennett et al., 1995) and a 3D a priori model of the crust and uppermost mantle and then damping the inversion according to the reliability of the a priori model (see below and Paffrath et al., 2021b, on inversion regularization). The purpose of the a priori model is to account for strongly heterogeneous velocity structure, particularly in the crust. In constructing their a priori crustal model, Paffrath et al. (2021b) discretize the EuCRUST-07 model of Tesauro et al. (2008) and the fully three-dimensional, high-resolution P-wave velocity model of Diehl et al. (2009) for the central Alpine region. In addition, information on Moho depth in the Alpine region is refined using the study of Spada et al. (2013).

The P-wave velocity at a given point in the a priori model is a weighted average of the Diehl and Tesauro models, with weights depending on the reliability of Diehl's model as measured by the values of the diagonal elements of the resolution matrix (RDE). For values of RDE above 0.15 the crustal model is dominated by Diehl's model, whereas for values below, the model of Tesauro et al. (2008) takes over smoothly (see Paffrath et al., 2001b, their Fig. 2 for the areas in which these models dominate). For regions of the inversion domain beyond the extent of the a priori crustal model, Paffrath et al. (2021b) assume the modified standard earth model AK135 of Kennett et al. (1995) and the 1D reference model used by Diehl et al. (2009). The advantage of this multifaceted approach is that it provides a comprehensive model of crust and mantle structure that allows for refined interpretation of the orogenic crust and its transition to the underlying mantle lithosphere, including subducted slabs.

Paffrath et al. (2021b) assess the resolution of mantle structures imaged in this study by employing different general tests, as well as very specific resolution tests that focus on crucial, smaller-scale structures in the Alps, e.g. gaps and different dip directions of slabs. Among the general tests are two checkerboard tests which regularly alter the velocity of the mantle in a synthetic model by applying a perturbation of $\pm 10\,\%$ in P-wave velocity on different cell sizes of $2 \times 2 \times 3$ grid points and $3 \times 3 \times 4$ grid points (Fig. 7 in Paffrath et al., 2021b). Gaps between the cells remain unperturbed in order to analyse smearing throughout the irradiated model domain.

Checkerboard tests show that, due to the uneven event distribution, smearing is more prominent in the NW–SE direction (Paffrath et al., 2021b, their Figs. 8–9). Hence, velocity anomalies in cross sections of slabs that dip in this vertical plane tend to be elongated in a down dip direction and lose amplitude, whereas structures trending perpendicular to this direction tend to be broadened along strike of the slab (Paffrath et al., 2021b, their Fig. 10). Generally, vertical smearing is greater at shallow depths and horizontal smearing increases with depth. Whereas the general recovery of the positions of the coarse checkerboard anomalies ($75 \times 75 \times 60$ km) is excellent down to the bottom of the inversion domain at 600 km, the amount of smearing increases with depth, decreasing the resolution below ~ 400 km to several tens of kilometres.

For smaller-scale anomalies ($50 \times 50 \times 45$ km), recovery of the pattern in checkerboard tests is impeded already below ~ 300 km depth, where smearing in the NW–SE direction as well as with depth becomes more significant. Also, the amplitude of these smaller anomalies decreases strongly at greater depths. Paffrath et al. (2021b) state that anomalies below 600 km depth marking the lower boundary of their inversion domain may be amplified and thus appear to lie above
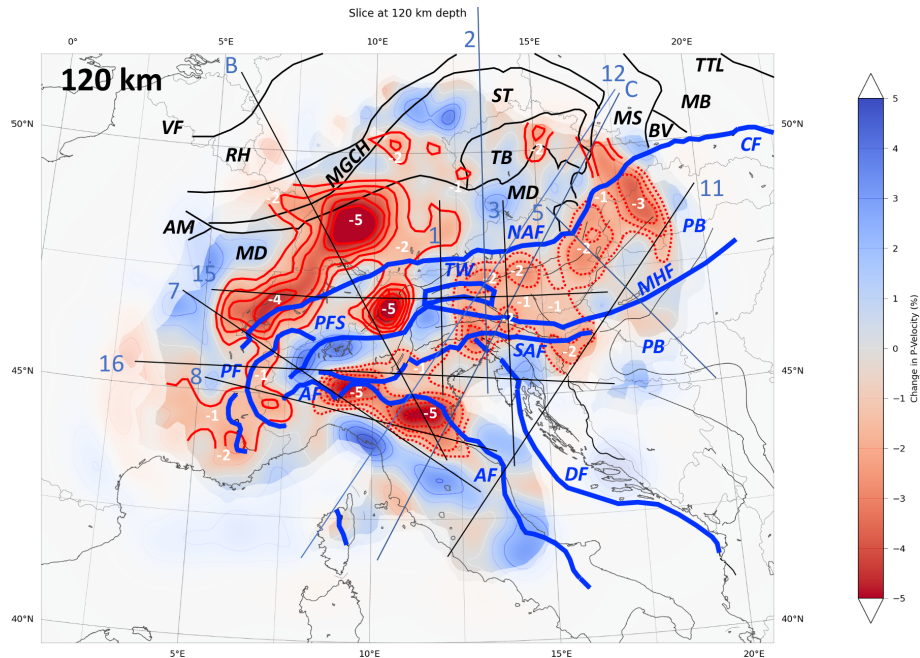
Figure 2. Horizontal V_p tomographic slice at 120 km depth in the mantle. Blue and red areas represent positive $(+V_p)$ and negative $(-V_p)$ anomalies, respectively. Contours of slow anomalies emphasized with thick red lines. Solid red contours – negative velocity anomalies interpreted as corresponding to pre-Alpine compositional domains; dashed red lines – negative velocity anomalies interpreted as corresponding to positive thermal anomalies in the mantle (see text for explanation). Thin black lines indicate the traces of all the profiles displayed in Figs. 3 to 6. Thick blue lines – main Alpine structures: NAF – Northern Alpine Front; SAF – Southern Alpine Front. Other Alpine structures and related features: PFS – Periadriatic Fault System; PF – Penninic Front; TW – Tauern Window; PB – Pannonian Basin; MHF – Mid-Hungarian Fault Zone; WCF – Western Carpathian Front. Thin black lines – Variscan boundaries: VF – Variscan orogenic front; RH – Rheno-Hercynian; MGCH – Mid-German Crystalline High; ST – Saxo-Thuringian; MD – Moldanubian; TB – Teplá–Barrandian; AM – Armorican Massif; BV – Brunovistulian; MB – Malopolska Block; MS – Moravo-Silesian. Other faults: TTL – Teysseyre–Thornquist Line.

this boundary. This is due to the hybrid approach of their tomography that only accounts for three-dimensional velocity perturbations within the inversion domain. To conclude this section, Paffrath et al. (2021b) show that their source–receiver set-up is able to distinguish fundamental differences in the geometry of slabs on the scale of tens to hundreds of kilometres, thus aiding us in interpreting these structures.

3 Observations of mantle velocity structure

For highlighting and interpreting the major mantle structures, we found it useful to trace contours of both positive and negative velocity anomalies in horizontal tomographic depth slices and then superpose these traces on the tectonic map of the Alps (Fig. 2) and compare them with anomaly contours in profiles across the orogen (Figs. 3–6). The surface locations of the aforementioned plate boundaries on these profiles are used as markers (e.g. Fig. 7). Also included in the profiles is the trace of the 7.25 km/s iso-velocity contour from the P-wave local earthquake tomography images of Diehl (2009). We use this contour as a proxy for the Moho in the entire Alps in lieu of other Moho models which are either local in their coverage (e.g. Behm et al., 2007; Brückl et al., 2007 in

the eastern Alps) or were found to provide inconsistent estimates of the Moho depth (Spada et al., 2013, e.g. in the Apennines and Ligurian region). The reader is referred to Kind et al. (2021) for a re-assessment of Moho depth. The Alpine crustal structure in the profiles is taken from cross sections of Schmid et al. (2004, 2013, 2017) and Cassano et al. (1986), whereas the pre-Alpine structure in the Alpine foreland is from Franke et al. (2017), Franke (2020), Mazur et al. (2020) and Schulmann et al. (2014).

A striking feature in horizontal slices at 100 to 220 km depth is the lateral continuity of $-V_p$ anomalies of up to 5 %–6 %, which reaches from the northern Alpine foreland across the Alpine orogenic front to beneath the western and central Alps as well as the westernmost part of the eastern Alps (Fig. 2, solid red contours). In three profiles crossing these parts (profiles B, 1 of Figs. 3b, c, 4a), $+V_p$ and $-V_p$ anomalies in the 100–220 km depth interval form coherent, inclined layers and together outline a package that dips beneath the Alpine front to below the centre of the orogen. In the next section, we explain why the base of this package is interpreted as being the base of the downward-moving European lithosphere, or lithosphere–asthenosphere boundary (LAB). This layered structure continues to down-dip to
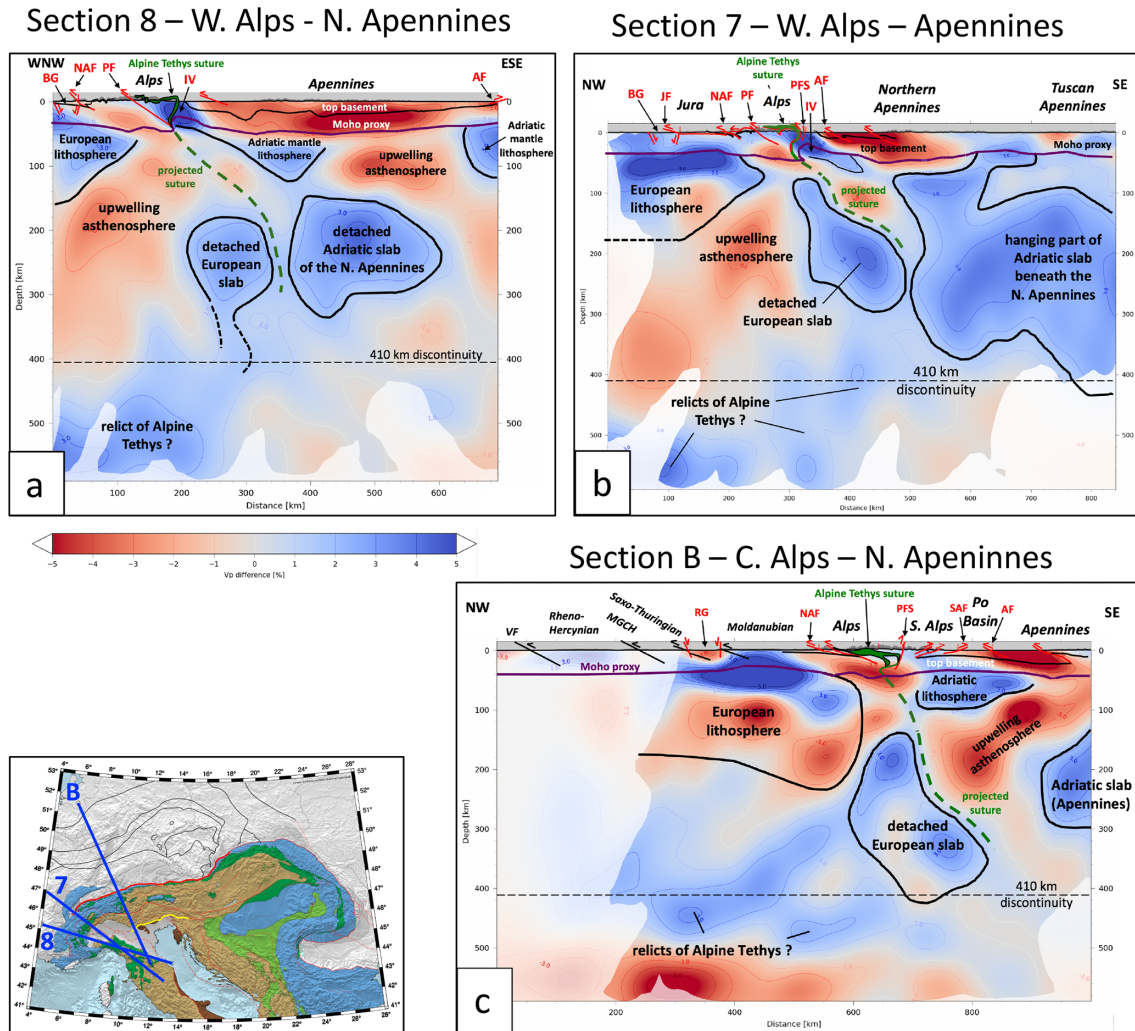
Figure 3. Cross sections of the western and central Alps along traces of profiles 8, 7 and B shown in inset: **(a)** western Alps; **(b)** western Alps from the Bresse Graben to the Northern Apennines, parallel to profile B of Lippitsch et al., 2003; **(c)** central Alps from the Variscan Belt to the Po Basin and Northern Apennines. Black solid lines: outlines of the European lithosphere, Adriatic lithosphere and detached to semi-detached slab material. Green dashed line – putative trace of Alpine Tethys suture based on the location of this suture in the schematic crustal cross sections depicted above the Moho proxy. The Moho proxy follows the V_p contour of $7.25 \, \mathrm{s^{-1}}$ obtained from the 3D crustal model of Diehl et al. (2009), part of the a priori model for obtaining crustal correction that was incorporated into the tomographic model (Sect. 2). Geological cross sections largely after Schmid et al. (2004, 2013, 2017) and Cassano et al. (1986); Variscan crustal cross sections after Franke (2017, 2000), Mazur et al. (2020) and Schulmann et al. (2014).

the southeast and beneath the core of the orogen, where it is interrupted (Figs. 3b, 4a). The putative location of the Alpine Tethys suture projected downward into the mantle in all profiles (dashed green line) is hypothetical and drawn in all profiles merely to show the affinity of the former Adria–Europe plate boundary to the European slab (see chapter 5). Profile 8 across the foreland of the southernmost western Alps (Fig. 3a) contains part of the Moldanubian core of the Variscan orogen (Franke et al., 2017) and differs from other profiles across the Alps in featuring only a high-velocity layer to some 150 km depth and dipping slightly beneath the front of the Alps.

Strong $-V_p$ anomalies of 3 %–5 % (contoured solid red in Fig. 2) generally underlie the central and western parts of the Moldanubian domain in the Alpine foreland and run somewhat oblique to the Variscan domain boundaries. They are not aligned with the Tertiary Bresse and Rhine grabens of Oligocene age (Fig. 1). Further to the east, in the area traversed by profiles 2 and 3 (Fig. 2), the subhorizontally oriented European lithosphere is characterized by dominantly positive velocity anomalies that cross beneath the front of the Alps and abut a low-velocity area in the central part of the Alps (see Fig. 4b, c; stippled red contours in Fig. 2). A large 2 % positive anomaly underlies the Moldanubian and

Teplá–Barrandian domains beneath the foreland of the eastern Alps, but does not extend beneath the orogenic front of the eastern Alps (Fig. 2; profiles 2 and 3 in Fig. 4b, c).

In the eastern Alps, the negative anomaly contours at 120 km depth in Fig. 2 (dashed red contours) form a broad maximum of 2 %–5 % in map view located between the Northern and Southern Alpine fronts and extending eastward from beneath the middle of the Tauern Window to the Pannonian Basin. Beneath the Eastern Alpine foreland, the upper 80–100 km are characterized by a broad, moderately positive V_p anomaly of 1 %–2 %. This eastern area shows no horizontal layering of $+V_p$ and $-V_p$ anomalies (profiles 2 and 3 of Fig. 4b, c), in contrast to the layering seen beneath the foreland in the profile immediately to the west (profile 1, Fig. 4a). The mantle structure beneath the core of the eastern Alps (profile 15, Fig. 5a) and beneath the transition to the Pannonian Basin (profiles 3 and 15, Figs. 4c, 5a) is marked by a shallow, strongly negative anomaly lid and, at depths between 150 and 400 km, by a strong, blob-like positive anomaly (5 %–6 %) surrounded by a negative anomaly and unconnected to the Alpine–Carpathian foreland (profiles 2, 3, 12 in Fig. 4b, c, 6a). The pronounced E–W change in anomaly structure below the core of the Alps is best seen in the orogen-parallel profiles (profile 15, Fig. 5a), where the 150–200 km thick positive–negative velocity layering characteristic of the central and western Alps gives way in the eastern Alps, more precisely beneath the western Tauern Window, to a negative anomaly extending down to about 130 km underlain by the deep (130–300 km) positive anomalies mentioned above. In the next chapter, we relate this orogen-parallel change to a first-order difference in the structure and composition of the subducted and delaminated slabs beneath the Alps.

The transitional area between eastern Alps and Western Carpathians (profile 5, Fig. 5b) and the Pannonian Basin (profile 11, Fig. 6b) is characterized by widespread $-V_p$ anomalies and by the almost complete absence of $+V_p$ anomalies above the 410 km discontinuity marking the top of the mantle transition zone. These $-V_p$ anomalies extend to the shallow mantle and directly underlie the 7.25 km/s Moho proxy marking the base of thinned orogenic crust. Weak $+V_p$ anomalies directly below the Moho are restricted to small parts of the Pannonian Basin (profile 11 in Fig. 6b). However, stronger $+V_p$ anomalies underlying the Moho are found beneath the Adriatic Sea (profiles 1, 2, 3 and 11, Figs. 4a–c, 6b), marking the still largely undeformed part of the plate of the same name.

Beneath the northern Dinarides (profile 11, Fig. 6b), no positive anomaly deeper than 100 km is observed. However, somewhat further to the north, beneath the northernmost Dinarides in Istria crossed by profile 16 (Fig. 5c), a generally northeast-dipping slab anomaly is fairly well resolved beneath the Dinaric Front, reaching a depth of about 140 km. Note that profile 16 is the same as that presented as profile M1 in Paffrath et al. (2021b).

A large, subvertically dipping positive anomaly directly below the Northern Apennines in profile 12 (Fig. 6a) is only connected to the crust near the Ligurian Sea and disconnected from the flat-lying high V_p mantle below the undeformed part of the Adriatic Plate further to the northeast. This Adria-derived slab dips down to the 410 km discontinuity. Further to the southeast beneath the Tuscan Apennines in profile 11 (Fig. 6b), this anomaly is completely disconnected from the orogenic crust and dips steeply to the southwest in a depth interval of 100–350 km. In a profile parallel to the Apennines (profile 7, Fig. 3b), this positive anomaly is seen to lose its connection with the orogenic crust between profiles 12 and 11 in Fig. 6a and b. Unfortunately, the resolution drops off to the southwest beneath the Ligurian and Tyrrhenian seas, but the faint anomalies in the former region suggest that the Moho proxy is directly underlain by a negative anomaly.

4   Choices in the interpretation of seismic structure

The tomographic profiles in Figs. 3–6 depict relative velocities as percentages of deviation from a mean velocity model for crust and mantle (Paffrath et al., 2021b). There are two main challenges in interpreting the anomaly patterns down to a depth of around 600 km:

1. distinguishing the effects of the present thermal state of the rocks from composition and structural anisotropy on the anomalies – this is difficult, if not impossible, in the absence of corroborative evidence from independent approaches, e.g. heat flow, gravity, conductivity and/or other seismological methods;

2. accounting for poor resolution of the tomographic images that often precludes a unique determination of the geometry of the anomalies – this is especially true of anomalies at great depth in the mantle, where vertical smearing blurs the images (Foulger et al., 2013).

Further headway in interpretation can be made by invoking geological criteria and what we broadly call "the geodynamic context" in order to weigh the consistency, and therefore the plausibility, of some interpretations over others. To illustrate this important point, we consider profile B across the central Alps in Fig. 3c, shown without interpretation in Fig. 7a and with two contrasting interpretations in Fig. 7b and c. This profile is a good place to begin our interpretative foray because the geology (i.e. structure, kinematics, metamorphism, thermal and stratigraphic ages) is well known along this classic section of the Alps (e.g. Schmid et al., 1996, 2004) and previous active-source seismology provides tight constraints on the crustal structure down to the Moho (Pfiffner and Hitz, 1997) and other sources in the NFP-20 volume (Pfiffner et al., 1997).

The uninterpreted profile B of Fig. 7a shows two main features: (1) the positive–negative anomaly layering extend-
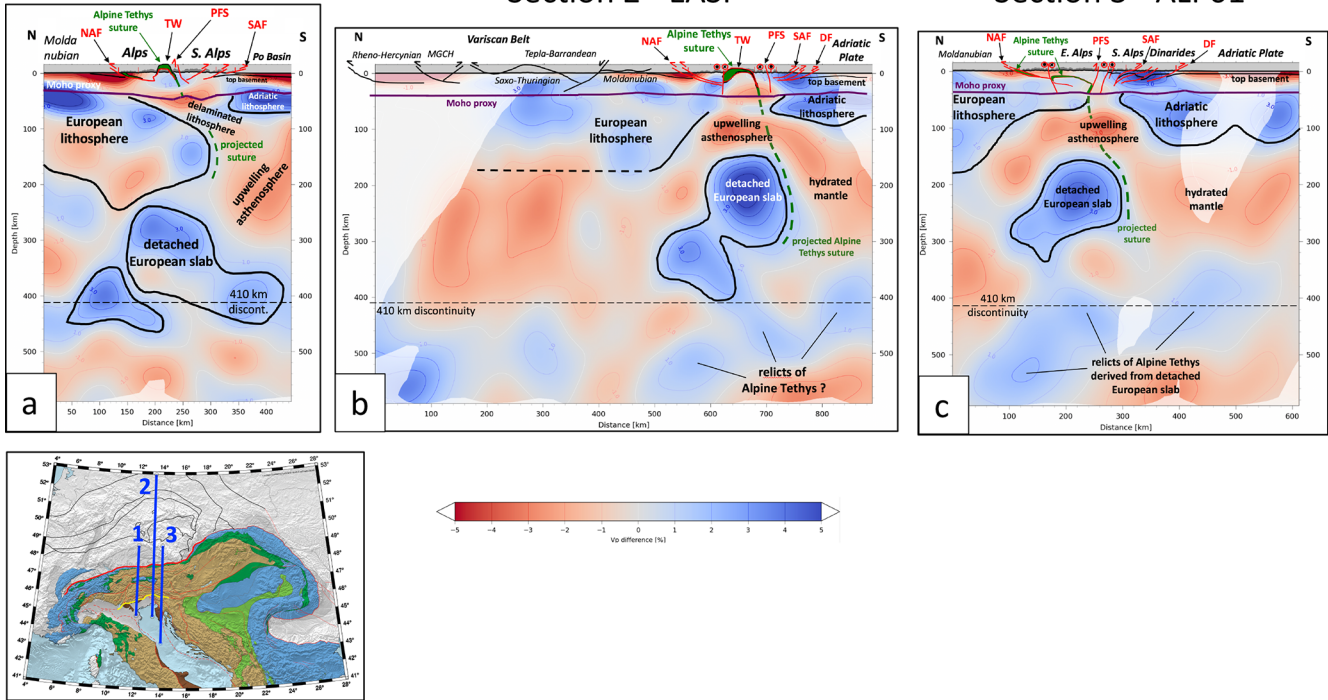
Figure 4. Cross sections of the eastern Alps along traces 1, 2 and 3 shown in inset. **(a)** Profile 1 (TRANSALP profile) from the Variscan foreland to the Po Basin. The thick European lithosphere has the same structure as beneath the central Alps (Fig. 3) and is partly detached. **(b)** Profile 2 (EASI profile) from the Variscan Belt to the Dinaric Front and Adriatic Plate. The base of the European lithosphere is mostly undefined seismically and the European slab is detached. **(c)** Profile 3 (ALP01 profile) from the Variscan Belt to the Adriatic Plate. See caption of Fig. 3 for further explanations. Alpine and related structures: NAF – Northern Alpine Front; SAF – Southern Alpine Front; PFS – Periadriatic Fault System; TW – Tauern Window; DF – Dinaric Front.

ing down to about 200 km observed in the Alpine foreland and extending to well south of the Northern Alpine Front down to 180 km depth, as described in the previous section, and (2) domains of deep-seated positive anomalies labelled with question marks, one dipping northward from the southern Alps down to the 410 km discontinuity below the Alpine foreland, a second minor one dipping southward below the Po Basin. In Fig. 7b, the positive–negative anomaly layering is interpreted as making up a coherent kinematic entity that moved as a unit with respect to the orogenic front and was subducted to the south–southeast beneath the Adriatic Plate in Tertiary times. A post-subduction age of this layering can be ruled out in the absence of a post Tertiary thermal event corresponding to the lateral extent of the $-V_\mathrm{p}$ anomaly in Fig. 2. The $-V_\mathrm{p}$ is therefore interpreted in Fig. 7b to form the bottom half of the lithosphere, i.e. the non-convecting part of the mantle.

We point out that not all plates in the greater Alps area comprise such thick, heterogeneous lithosphere. Indeed, as shown in the next section, the Adriatic Plate and the Adria-derived slab beneath the Apennines comprise lithosphere in the standard sense of a seismically "fast", more homogeneous kinematic entity.

The slab of thick lithosphere descending beneath the Northern Alpine Front in Fig. 7b is interpreted as being broken, with its fragment continuing down to the 410 km discontinuity beneath the Po Basin. Weaker positive anomalies beneath the Alps in the 300–600 km depth interval may be subducted and detached relics of the Alpine Tethyan Ocean. However, resolution is poor at these depths, so our interpretation of such relics is speculative, as indicated by question marks in the figures.

In the interpreted profile B (Fig. 7b) other $-V_\mathrm{p}$ anomalies in the mantle occur immediately beneath the Moho in the cores of the Alps and Apennines where the Moho lies at ca. 50 km depth and where the lower crust is also characterized by low V_p. Finally, a deep-seated $-V_\mathrm{p}$ anomaly is found below the Adriatic lithosphere, between the detached part of the European slab and the Northern Apennines slab derived from Adriatic lithosphere (Fig. 7b). In the former case, the $-V_\mathrm{p}$ anomaly in the mantle immediately below the Moho is interpreted as manifesting a depression of the absolute velocities by the occurrence of hydrous, less dense and therefore seismically slower material in the subduction channel. In the case of the deep-seated $-V_\mathrm{p}$ anomaly labelled "upwelling asthenosphere", the negative anomalies of
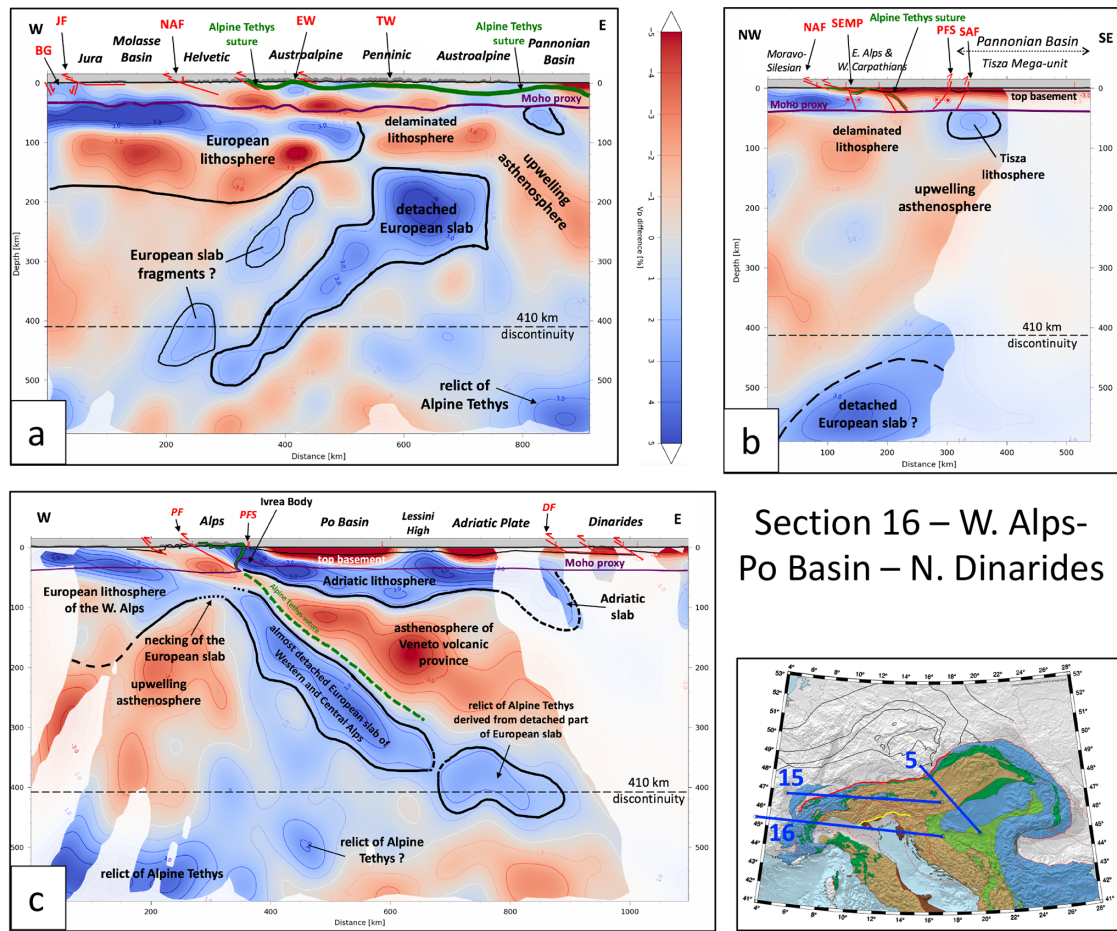
Figure 5. Cross sections of the Alps along traces 15, 5 and 16 shown in inset. **(a)** Orogen-parallel profile 15 from the central Alps across the eastern Alps to the Pannonian Basin; note the decrease in thickness of the European lithosphere before its delamination from the crust at and east of latitude 12° E crossing the area of the western part of the Tauern Window (TW). **(b)** Profile 5 from the Variscan Belt in the northwest to the Pannonian Basin in the southeast across the transitional area between eastern Alps and Western Carpathians. The European lithosphere has completely delaminated during Neogene stretching in the greater Pannonian area that formed a back-arc basin in the upper plate consisting of the ALCAPA and Tisza mega-units during Carpathian rollback subduction. See caption of Fig. 3 for further explanations. **(c)** Profile 16 from the western Alps across the Po Basin to the northern Dinarides (same as profile M1 in Paffrath et al., 2021b); note the apparent dip of the still attached European slab beneath the western and central Alps as well as the trace of a slab of Adriatic lithosphere under the northern Dinarides.

up 5 %–6 % could possibly be caused by still hot, upwelling asthenosphere. However, as argued in Sect. 6.3, this would need a ΔT of some 600–700°C resulting in temperatures well above 1400°C. Following the suggestion by Giacomuzzi et al. (2011), we envisage hydrated, possibly decarbonated mantle (Malusà et al., 2018, 2021) in a back-arc position behind the descending non-detached and detached parts of the European lithosphere rather than still existing, substantially elevated temperatures as a suitable explanation for the low V_p in this area.

In the contrasting interpretation shown in Fig. 7c, all anomalies are considered primarily to reflect temperature anomalies, such that positive anomalies at depths below the Moho are interpreted as subducted lithosphere, whereas negative anomalies below the Moho are equated with hot asthenosphere and are not part of a subducted plate. This is in line with the thermo-rheological definition of a descending sheet of rigid and cold lithosphere. Thus, the base of the positive anomaly extending from the European foreland to below the Northern Alpine Front would mark a descending lithospheric plate only 80 km thick, whereas the long north-dipping, positive anomaly domain in this profile could be interpreted as subducted Adriatic lithosphere connected to Adriatic lithosphere beneath the Po Basin and the Adriatic Sea (Fig. 7c). If true, this would imply a thin European continental lithosphere and necessitate hundreds of kilometres of
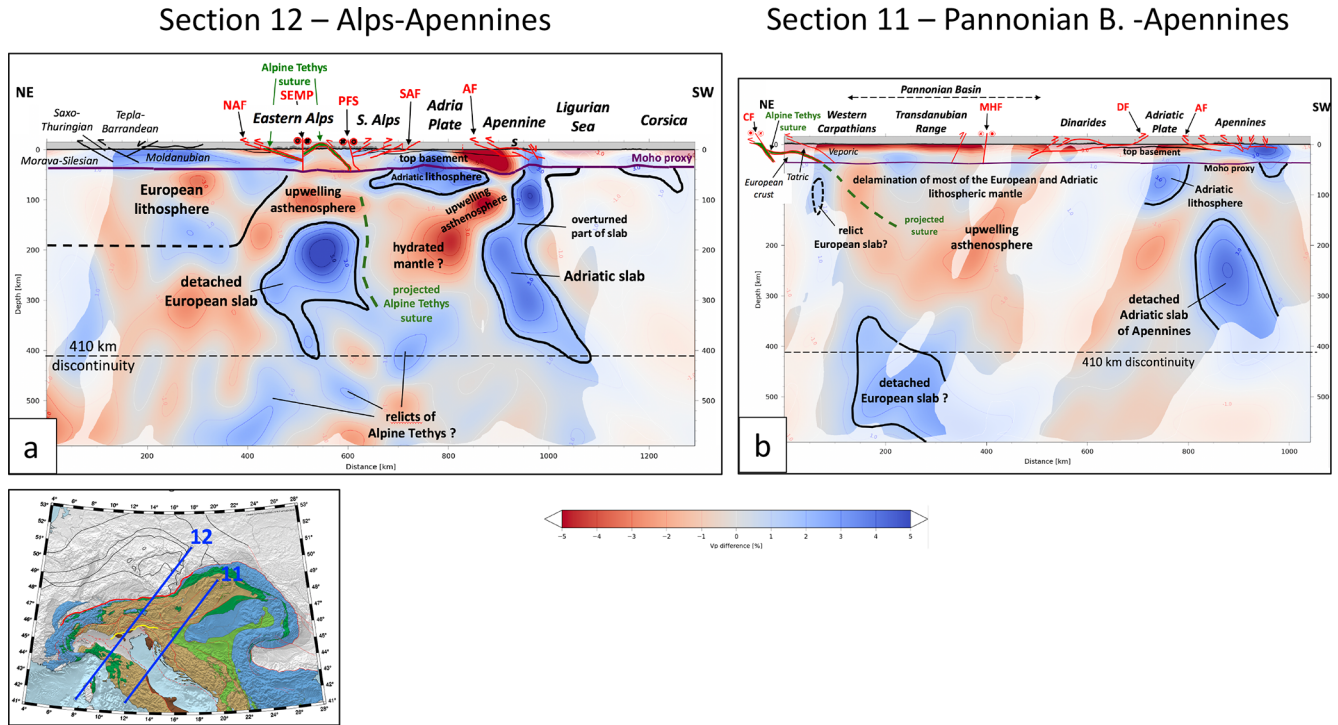
Figure 6. Profiles 12 and 11 along traces shown in Figs. 1 and 2 across the greater Alpine area, Adria and the Apennines. **(a)** Profile from the Variscan Belt across the eastern Alps to the Northern Apennines and the Ligurian Basin. The European slab beneath the Alps is detached, whereas the Adriatic slab beneath the Apennines hangs subvertically and is partly overturned (see text). **(b)** Profile from the Central Western Carpathians across Pannonian Basin, northern Dinarides, Adriatic plate, Central Apennines to the Tyrrhenian Sea. The European lithosphere is completely delaminated, the Adriatic slab beneath the Dinarides is almost absent, and the Adriatic slab beneath the Apennines is detached from a remnant of the Adriatic lithosphere beneath the Adriatic Sea. See caption of Fig. 3 for further explanations. Alpine faults and related structures (labelled red): NAF – Northern Alpine Front; SAF – Southern Alpine Front; PFS – Periadriatic Fault System; SEMP – Salzach–Ennstal–Mariazell–Puch Fault; MHF – Mid-Hungarian Fault Zone; CF – Carpathian Front; DF – Dinaric Front; AF – Apennine Front.

shortening in the Alps within predominantly S-facing folds and thrusts for which there is no geological evidence. Most folding and thrusting in the Alps is N- to NW-vergent, as documented by more than a century of detailed study. Within the southern Alps where S-vergent thrusting is indeed observed, only about ≤ 72 km of shortening was accommodated, mostly in Oligo-Miocene times (Schönborn, 1992; Schmid et al., 1996; Rosenberg and Kissling, 2013). This effectively precludes any scenario involving north-directed subduction of large amounts of Adriatic lithosphere beneath the Alps. Moreover, the continuity of the NW-dipping $+V_p$ anomaly in Fig. 7c may reflect smearing, which is prevalent in profiles with this azimuthal orientation (see Sect. 2 above).

This leaves Fig. 7b with its anomalously thick (180–200 km) subducting European lithosphere as the preferred interpretation. The total length of subducted European slab according to the interpretation in Fig. 7b is roughly 400 km, as measured between the Northern Alpine Front down to the 410 km discontinuity (see also profile 6 in Appendix A1). This is consistent with the amount of shortening in the Alps since European lithosphere entered the subduction zone in

the Alps in Eocene times (Schmid et al., 1997; Handy et al., 2010), lending further support to our interpretation. We return to this point in Sect. 6 below.

5 Regional tectonic interpretation

In interpreting the images in Figs. 3–6 and all the additional profiles in Appendix A, we marked boundaries (thick black lines) around kinematically coherent images whose geometry is consistent with available data on Moho depth and with the kinematic history of tectonic units exposed at the surface. Dashed solid black lines delimit very poorly defined or even putative boundaries. The base of the European foreland lithosphere in the central Alps is well defined and taken to be the base of the $-V_p$ layer at about 180 km depth, as discussed in the previous section (profiles 1, 4, 6, 9, 15 and B in Appendix A). In other profiles, especially in the eastern Alps where the base of the lithosphere is poorly defined, we placed the lower boundary at approximately the same 180–200 km depth to avoid abrupt along-strike variations in lithospheric thickness beneath foreland crust with the same
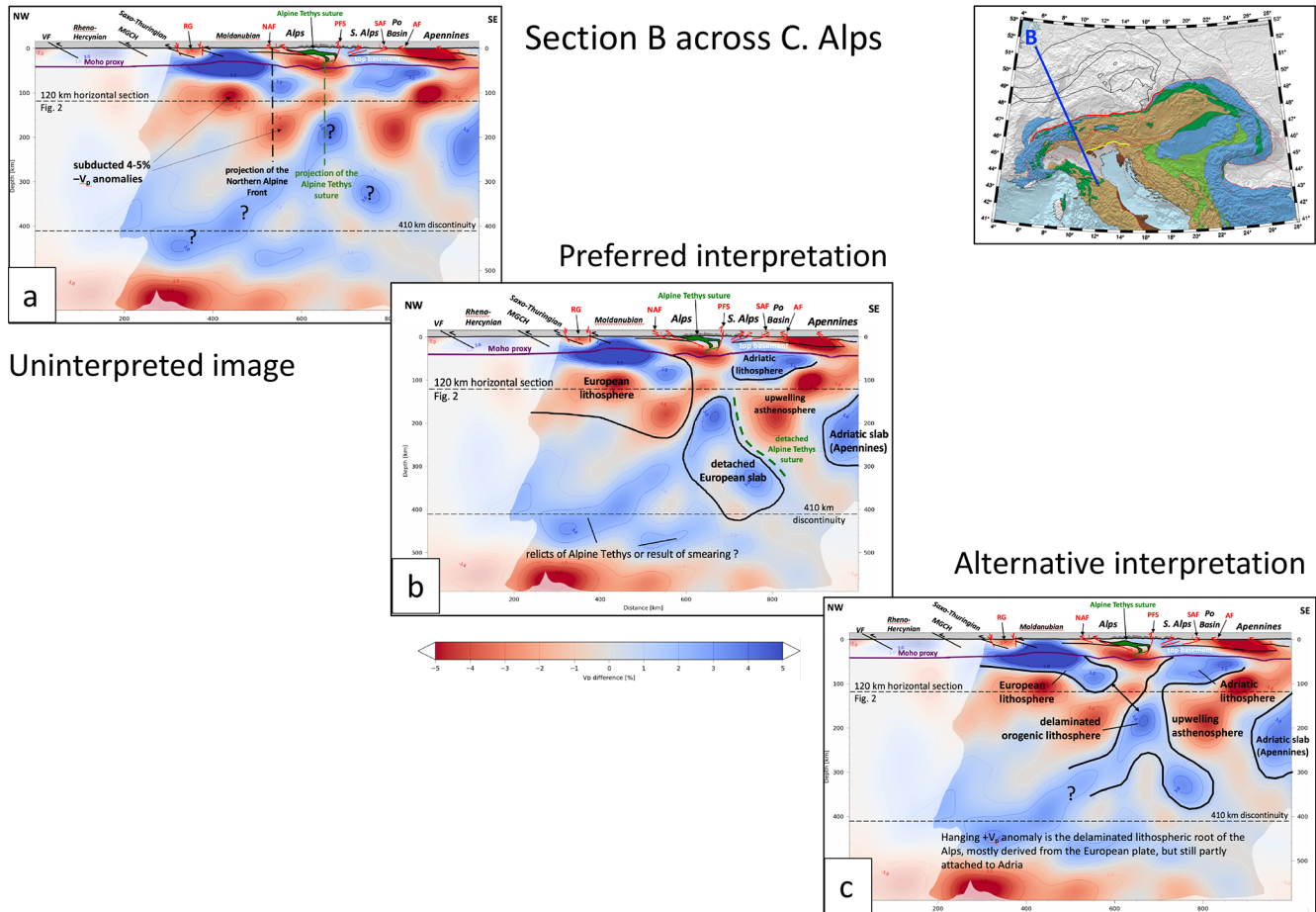
Figure 7. Raw image of vertical tomographic profile B across the central Alps and two alternative interpretations. **(a)** Raw image showing layered positive and negative V_p anomalies extending from the Variscan Belt to south of the Northern Alpine Front (NAF, see also Fig. 2). **(b)** Preferred interpretation shown in Fig. 3c, indicating coherence of layered positive and negative V_p anomalies that are interpreted as thick and old (Variscan or older?) European lithosphere dipping to the south beneath the Alps. The European slab is detached. In contrast, the Adriatic lithosphere beneath the Po Basin and Apennines is thin and underlain by a large negative anomaly interpreted as upwelling asthenosphere. **(c)** Standard interpretation of lithosphere as comprising only positive V_p anomalies, thought to be old, cold lithosphere. The long N-dipping positive V_p anomaly is interpreted as the delaminated lithospheric root of the Alps, mostly derived from the European Plate but still partly attached to the Adriatic Plate (see text for discussion).

Variscan and pre-Variscan history. Thus, some boundaries are drawn across seismically fast and slow domains, highlighting the difficulty of using solely seismological criteria to define the LAB (Artemieva, 2011). In Figs. 8 and 9, we include two horizontal depth slices at 240 and 90 km, respectively, to show the main structures outlined by velocity anomalies in map view.

5.1 Alps

European lithosphere of Variscan and/or pre-Variscan origin originating in the Alpine foreland is evident in all cross sections of the central Alps (Figs. 3, 4), though its base in the eastern Alps is undefined (e.g. profile 2 in Fig. 4b). Beneath the central Alps and westernmost eastern Alps, this lithosphere dips to the south to become the thick, subducted European slab (profiles B and 1 in Figs. 3c, 4a), whereas in the western Alps (profiles 8 and 7 in Fig. 3a, b) and in the eastern Alps east of 12° E (profiles 2, 3 and 12 in Figs. 4b, c, 6a), the European slab is completely detached from its foreland. Only in the transitional area between western and central Alps is the slab still tenuously connected to the European lithosphere of the Alpine foreland (profile 16, Fig. 5c). The moderate dip and inordinate length of the slab beneath the entire E–W extent of the Po Basin in this particular profile reflect the fact that this W–E-running profile obliquely slices the European slab at a high angle to the SE dip of Alpine subduction in the western and central Alps. Moreover, the E-dipping positive anomaly seen in Fig. 5c comprises different pieces, with the positive anomaly at the eastern end (below the Adriatic plate east of the Lessini Mountains, at a depth of around 350–
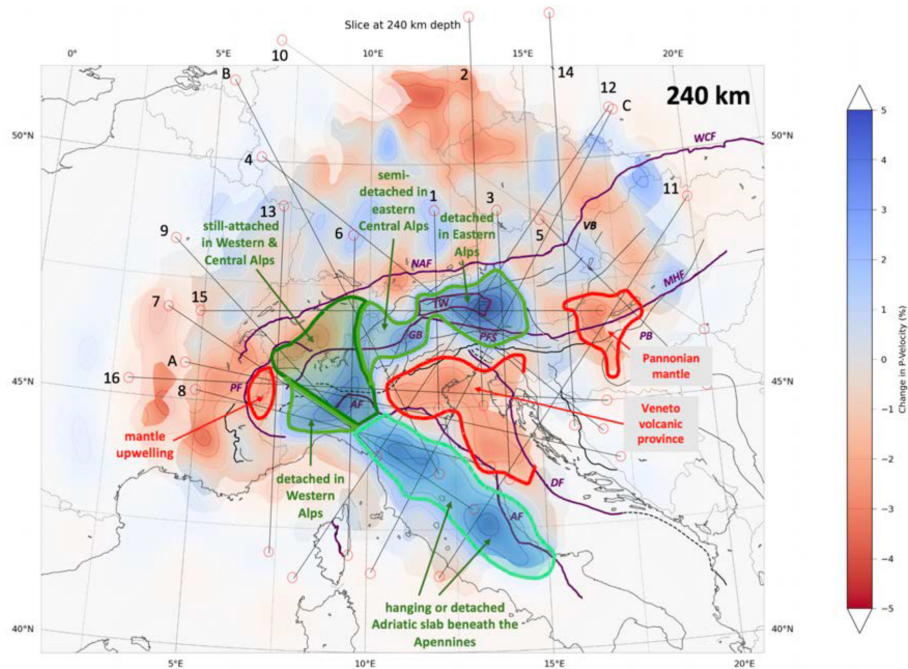
Figure 8. Horizontal V_p tomographic slice at 240 km. Blue and red areas represent fast and slow teleseismic P-wave anomalies, respectively. Isolines indicate deviation in percentage of P-wave velocities from the mantle model in Paffrath et al. (2021b). Green lines are boundaries of slabs at their intersection with the horizontal plane of the depth slice. The slab boundaries were obtained by projecting the interpreted slab outlines marked with black lines in the 19 profiles in Appendix A (traces shown as thin black lines) into the plane of the depth slice. Shades of green denote various degrees of attachment of the European slab to the European lithosphere in the Alpine foreland (see interpreted profiles and text). Red lines outline domains of mantle upwelling. Thick black lines are major Alpine faults: NAF – Northern Alpine Front; PFS – Periadriatic Fault System; GB – Giudicarie Belt; PF – Penninic Front; TW – Tauern Window; VB – Vienna Basin; PB – Pannonian Basin; MHF – Mid-Hungarian Fault Zone; AF – Apennines Front; DF – Dinaric Front.

450 km) originating from a south-dipping slab fragment below the eastern Alps depicted in Fig. 4a. This easternmost part of the positive anomaly in profile 16 of Fig. 5c also slices minor, discontinuous relics of Alpine Tethys south of the main slab in the eastern Alps (see lower right-hand side of N–S-trending profile 2 in Fig. 4b).

In the western Alps, detachment of the European slab (Fig. 3a, b) was previously noted by Lippitsch et al. (2003) and interpreted as a subhorizontal tear that is currently propagating from southwest to northeast towards the still attached part of the slab in the western central Alps (Kissling et al., 2006). The detachment of this part of the slab (profile A in Appendix A), possibly combined with unloading due to glacial erosion and melting (Champagnac et al., 2007; Mey et al., 2016), has been deemed responsible for rapid Plio-Pleistocene exhumation and surface uplift of the western Alps (Fox et al., 2015, 2016), which have the highest peaks (up to 5000 m) and greatest relief (3000 m) of the entire Alpine chain.

In the eastern Alps, the detached European slab hangs subvertically to steeply N-dipping in a depth interval ranging from 150 to 350–400 km. We note that the pronounced along-strike change in orogenic mantle structure between

nearby profiles 1 and 2 (Fig. 4a, b) does not coincide with the Austroalpine–Penninic boundary marking the Alpine Tethys suture between the central and eastern Alps at the surface. This along-strike change is best seen by comparing the mantle structure in an orogen-parallel profile with the location of the suture in the tectonic map (profile 15 in Fig. 5a) and its projected trace in the horizontal depth slice at a depth of 90 km (Fig. 9). Rather, it coincides with the northward projection of the Giudicarie Belt (marked GB in Fig. 1), a post-collisional fault of latest Oligocene to Miocene age (Pomella et al., 2012) which sinistrally offsets the eastern and southern parts of the Alpine orogenic edifice, including the Periadriatic Fault System (Verwater et al., 2021). The northward projection of the Giudicarie Belt, which lies in the Tauern Window in map view, coincides with the westernmost point of eastward, orogen-parallel extrusion of the Alpine and Western Carpathian lithosphere in latest Oligocene to Miocene times (e.g. Scharf et al., 2013; Schmid et al., 2013; Favaro et al., 2017). This allochthonous block is referred to in the literature as the ALCAPA mega-unit. The orogenic Moho beneath this block shallows dramatically to the east (e.g. Grad et al., 2009; Kind et al., 2021), reaching a depth of some 20 km beneath the Pannonian Basin (profiles 15 and 5 in
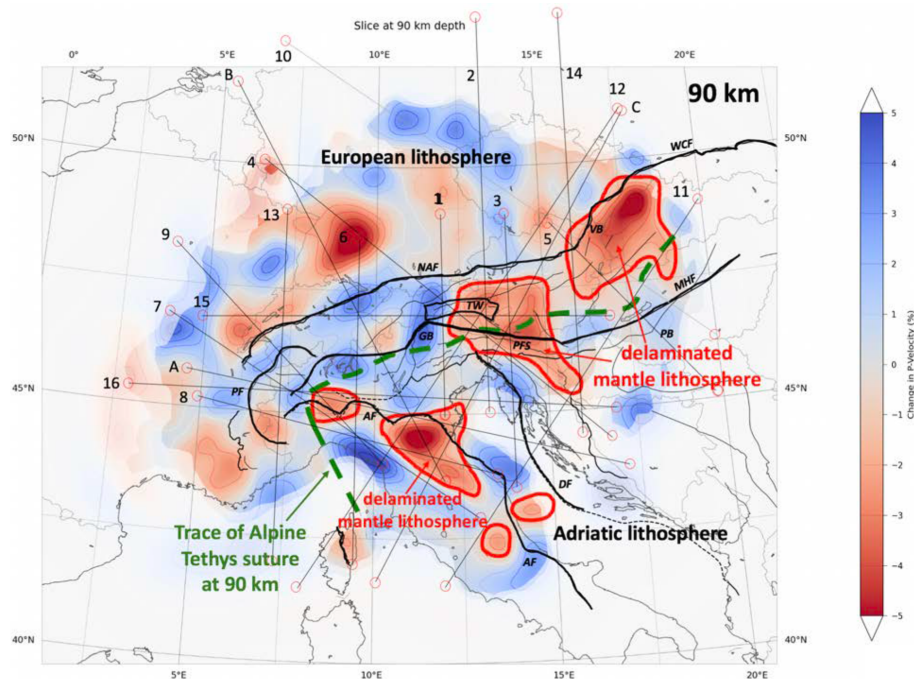
Figure 9. Horizontal V_p tomographic slice at 90 km depth. Blue and red areas represent fast and slow teleseismic P-wave anomalies, respectively. Isolines indicate deviation in percentage of P-wave velocities from the mantle model in Paffrath et al. (2021b). Thick dashed green line is the projection of the suture zone of Alpine Tethys down to 90 km based on interpretation of the profiles. This green line marks the southern boundary of the European Plate with the Adriatic Plate and the lithosphere of the Tisza mega-unit beneath the Pannonian Basin. Note the variable P-wave velocities within the European lithosphere at this depth due to pre-Alpine tectogenesis. Areas outlined in red indicate areas with low V_p located within the Alpine-age orogens where shallow asthenosphere replaced delaminated mantle lithosphere after slab detachment in the Alps, Western Carpathians and the Apennines occurred.

Fig. 5a, b). The occurrence of negative V_p anomalies and reduced gravity anomalies (Zahorec et al., 2021) immediately below this shallow orogenic Moho in the eastern Alps (e.g. profile 12, Fig. 6a, highlighted low-V_p area in Fig. 9) strongly suggests that the entire lithospheric mantle reaching from the Tauern Window of the eastern Alps to their transition with the Western Carpathians (profile 5 in Fig. 5b) has been delaminated.

5.2 Pannonian Basin

The negative V_p anomaly of the eastern Alps continues further to the northeast to beneath the Vienna Basin and the central Western Carpathians, as seen in the 90 and 120 km depth slices (Figs. 2, 8). This is the area overlying slab remnants that have descended into the mantle transition zone (e.g. profile 5 in Fig. 5b). The Central Carpathians host a province of 17–14 Ma post-collisional sub-alkaline magmatism (Seghedi and Downes, 2011; Seghedi et al., 2013) related to Miocene extension of the Pannonian domain in the upper plate of the Western Carpathian orogen. Given the fact that this magmatism ended some 14 Myr ago, it is uncertain if the low V_p anomaly in the Western Carpathians is solely related to a persistent positive thermal anomaly. In this context, it is relevant

to note that the area of the Tisza mega-unit south of the Mid-Hungarian Shear Zone (MHZ in Fig. 1) and characterized by high heat flux (Horvath et al., 2015, their Fig. 12) does not exhibit such a negative V_p anomaly. This indicates that present-day heat production does not correlate with negative seismological anomalies everywhere.

Relics of delaminated and detached European lithosphere can be detected at and below the 410 km discontinuity beneath the Pannonian Basin (profiles 5 and 11 in Figs. 5b, 6b) as previously discovered in the passive array swath experiment of Dando et al. (2011). As mentioned in discussing Fig. 7, the 400 km down-dip length of the slab segments is broadly consistent with estimates of shortening since the European slab entered the subduction zone after the closure of Alpine Tethys at around 40 Ma (e.g. Schmid et al., 1996; Handy et al., 2010; Kurz et al., 2008). This suggests that the detached slab remnants comprise mostly European lithosphere (Mitterbauer et al., 2011; Rosenberg et al., 2018; Kästle et al., 2020).

5.3 Adriatic Plate

The Adriatic Plate is 100–120 km thick as defined by the lower limit of the horizontal $+V_p$ anomalies beneath the
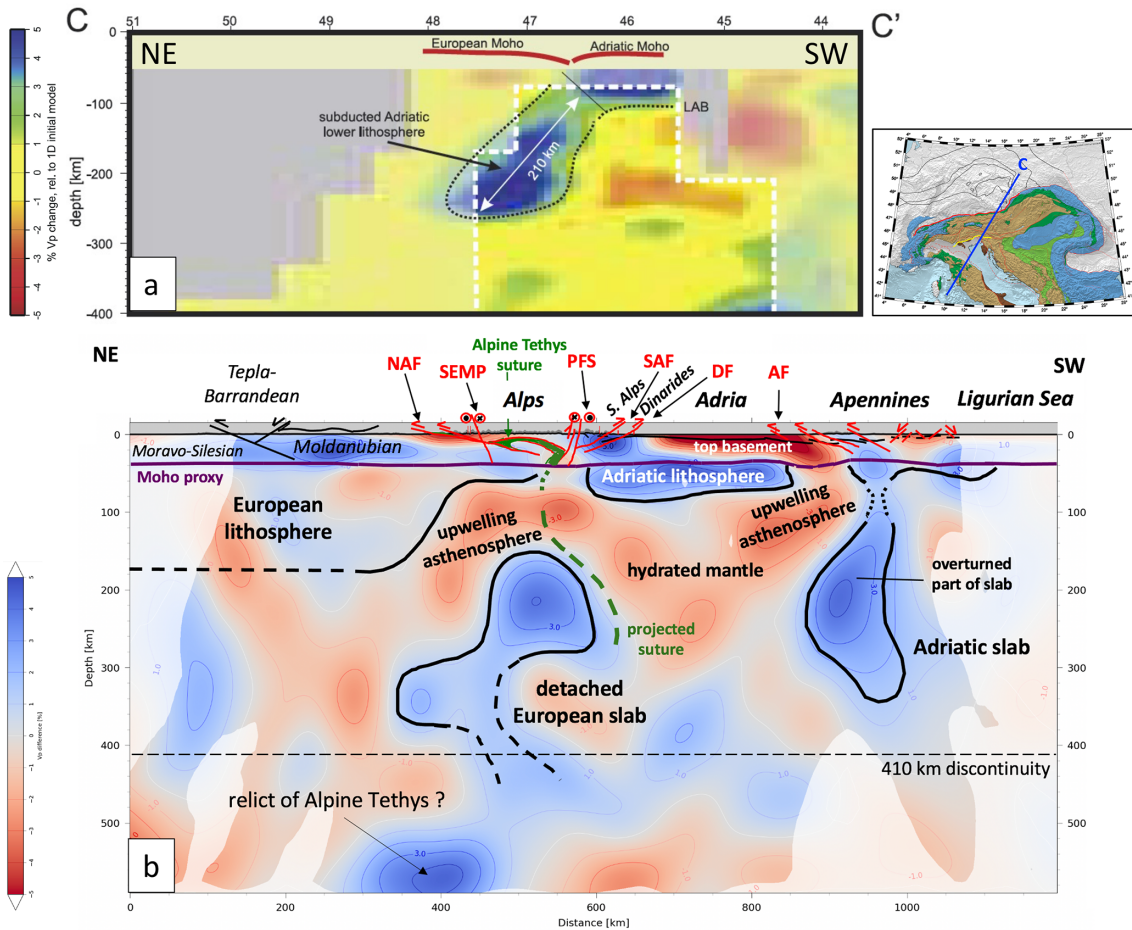
Figure 10. Two tomographic profiles along the trace of profile C (given in inset map) on the same scale: **(a)** Lippitsch et al., 2003; **(b)** this work. The profiles show moderate agreement regarding slab detachment beneath the eastern Alps but disagreement regarding the dip and length of the slab anomaly. Our preferred model in **(b)** provides evidence of the delamination of most of the underpinnings of Adria and Europe beneath the Alps, Adria and Apennines. A direct connection of the NE-dipping slab beneath the eastern Alps to the Adriatic lithosphere shown in **(a)** becomes untenable in light of the new data presented in **(b)**.

Adriatic Sea. We label this the Adriatic lithosphere and regard it as Adriatic lithosphere in a kinematic sense (e.g. profiles 1, 2, 3 and 12 in Figs. 4, 6a). This is less than half the thickness of the European lithosphere. It is generally accepted that in the Alps the former Adriatic Plate formed the upper plate during convergence, whereas in the Dinarides and Apennines, Adria is the subducting plate. The Adriatic slab in the Apennines possibly has a simpler velocity structure than the European slab in the Alps, comprising thinner and compositionally more homogeneous lithosphere with only $+V_p$ anomalies (Fig. 6). In contrast to the European foreland (Franke, 2020), most of the former Adriatic Plate was not affected by high-grade metamorphism and never experienced the closure of various Paleozoic oceans. Instead, it has been interpreted as the southern, Gondwana-derived foreland of the Variscan belt (Molli et al., 2020).

The Adriatic lithosphere is underlain by a pronounced low-velocity mantle in depth interval of 150–350 km (pro-

files B and 3 in Figs. 3c, 4c, right-hand side; profile 12 in Fig. 6; profiles B, 3, 12, 11 in Appendix A). This thick low-velocity zone coincides at the surface in the eastern Po Basin and northern Adriatic Sea with the Veneto volcanic province (Figs. 1, 8), which comprises mostly primitive basalts diluted by a depleted asthenospheric mantle component (Macera et al., 2003). Its age range between late Paleocene to late Oligocene (Beccaluva et al., 2007) spans the transitional time from subduction to collision in the Alps (Handy et al., 2010, and references therein). It is thus tempting to attribute this magmatism to the combined effects of heat and fluid advection behind the originally S-dipping European slab in the Alps (Macera et al., 2008). The release of water and incompatible elements from deeply buried sediments along the slab interface may have caused hydration of the overlying mantle, giving rise to an overall decrease in seismic velocity, as proposed by Giacomuzzi et al. (2011) to explain the negative anomaly layer beneath the Adriatic Plate.
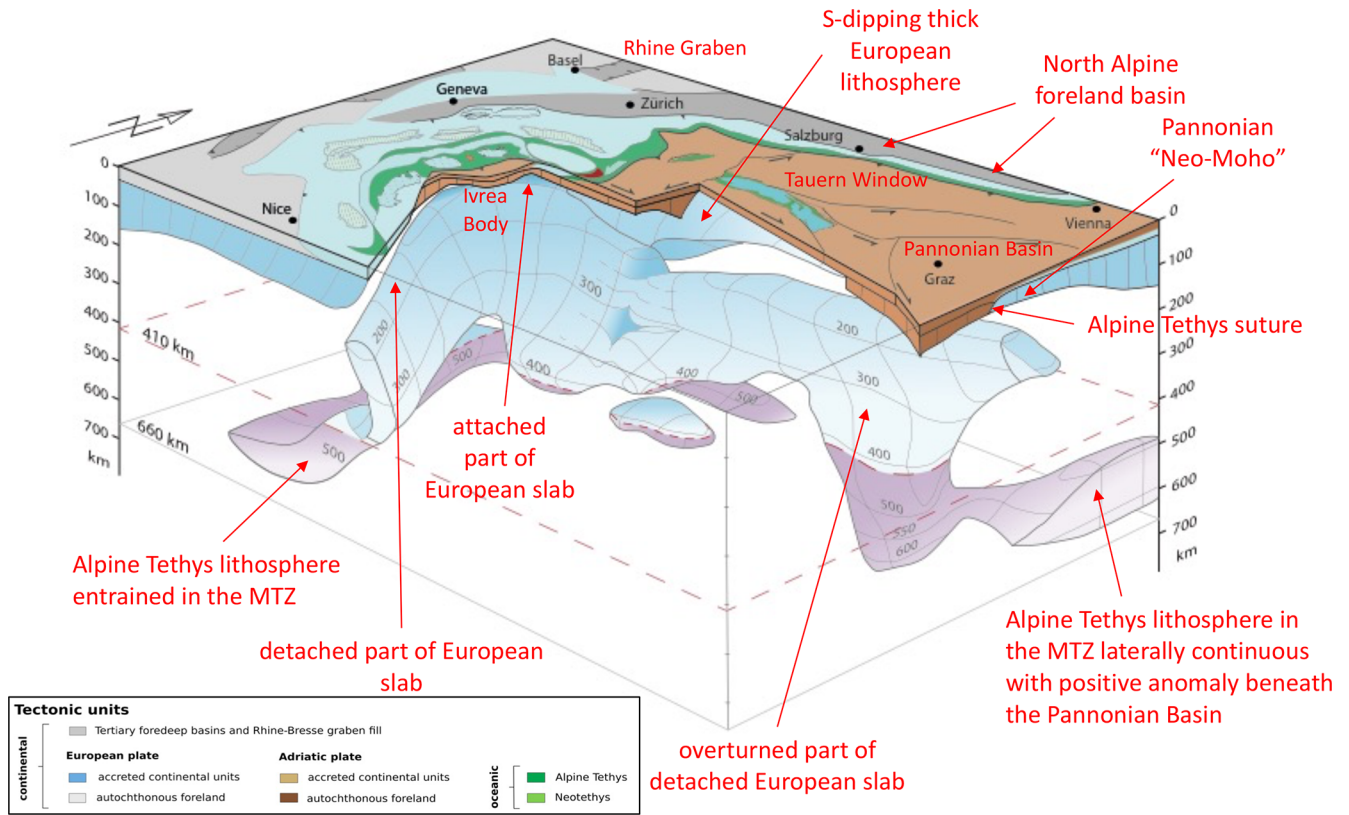
Figure 11. Three-dimensional diagram of the slab beneath the Alps as viewed from the southeast. Slab geometry based on projections of all vertical tomographic profiles in Appendix B and horizontal sections from the model of Paffrath et al. (2021b). Tectonic map of the surface is simplified from maps of Schmid et al. (2004) and Schmid et al. (2008).

5.4 Apennines

Switches in the polarity of subduction are manifested at the surface by changes in thrust vergence and location of the orogenic fronts at the Alps–Apennines and Alps–Dinarides junctions (Fig. 1). The mantle structure at the Alps–Apennines junction is simpler than the complex surface fault structure due to switching subduction polarity (Molli et al., 2010; Schmid et al., 2017) would suggest. There, the European and Adriatic slabs are easily distinguished in profiles 8 and 7 (Fig. 3a, b). In the horizontal slice at 240 km depth in Fig. 8, the two slabs cannot be distinguished at the resolution of the horizontal depth slice because they are very close to each other (see Fig. 3a, b). However, the horizontal slice at 90 km (Fig. 9) shows them separated by the downward projection of the Alpine Tethys suture. Note that the European slab beneath the western and central Alps was subducted to the southeast below the Adriatic Plate prior to 35 Ma, ultimately leading to the Alpine Tethys suture depicted in Fig. 9. Adria–Europe suturing occurred before the Apennines formed in latest Oligocene to Miocene and Pliocene times. When considering profiles 8 and 7 in Fig. 3a, as well as profiles 12 and 11 in Fig. 6a and b in the following discussion, it is important to note that

the Adriatic slab beneath the Northern Apennines originally dipped to the southwest when it was still attached to the then still undeformed western part of the Adriatic Plate (Facenna et al., 2004; Schmid et al., 2017). Apenninic orogenesis involved E-directed rollback of this former Adriatic Plate that currently makes up the slab below the Northern Apennines.

In profile 12 (Fig. 6a) across the Northern Apennines, the upper 200 km of the Adriatic slab anomaly dips to the northeast and is hence overturned, as pointed out in Sect. 3. This slab is detached from the Adriatic lithosphere and located in the NE foreland of the Apennines. Somewhat more to the south in profile 11 (Fig. 6b) across the central (Tuscan) Apennines, the Adriatic slab is normally inclined, i.e. dips to the southwest, and completely detached from the orogenic wedge of the Apennines. In profile 7 (Fig. 3b) running parallel to the strike of the Apennines slab, a subhorizontal tear is clearly visible beneath the Tuscan Apennines at a depth of 80–100 km. We speculate that once the Apennines stopped advancing in Plio-Pleistocene times (e.g. Molli et al., 2010), the heavy Northern Apennines slab steepened. The subhorizontal tear visible in Fig. 3b appears to have propagated from southeast to northwest, i.e. in a direction of decreasing orogen-normal shortening in the Apennines and towards the pole for Neogene anticlockwise rotation of the

Corsica–Sardinia block with respect to Europe (Speranza et al., 2002), also affecting the Apenninic orogen (Maffione et al., 2008). Partial tearing allowed the detached part of the slab in the southeast to retreat and sink under its own weight, while the smaller, still partly attached segment in the northwest became vertical and locally overturned (profile 12 in Fig. 6a). The maximum depth (8–9 km) of Plio-Pleistocene fill in the Northern Apenninic foreland or "Po" Basin (Bigi et al., 1989) and the deepest Moho beneath the Northern Apennines (50–60 km, Spada et al., 2013) are both attributed to the downward pull of this still partially attached slab segment depicted in profile 12 of Fig. 6a (Picotti and Pazzaglia, 2008).

The horizontal depth slice at 90 km in Fig. 9 shows the area traversed by profiles 12 and 11 discussed above that is characterized by low V_p and interpreted as outlining lithospheric delamination during slab detachment. These areas extend from northwest to southeast along the front of the NE-facing Apennines nappe stack. This indicates that the Adriatic slab below the Apennines has detached from the little-deformed Adriatic Plate in the Adriatic Sea almost all along the strike of the Northern and Central Apennines. Note that this area of delamination is slightly NE of the outline of the detached and subvertical Adriatic slab shown in the horizontal depth slice at 240 km depth (Fig. 8).

5.5 Dinarides

Our data only cover the area of the northern Dinarides and the Dinarides–Alps junction in Slovenia (Stipčević et al., 2011, 2020). Collisional shortening after the closure of the Neotethyan oceanic tract in the northern Dinarides started earlier than in the Alps; major collisional shortening lasted from Late Cretaceous to Oligocene times, with only very minor shortening in the Miocene (e.g. Schmid et al., 2008). In the Alps, collisional shortening after the closure of Alpine Tethys started later, namely in the late Eocene, and lasted until Pliocene times. The junction between the Alps and the Dinarides is marked at the surface by the Southern Alpine Front that thrust the southern Alps southward over older NW–SE-striking Dinaric thrusts (Fig. 1) in the late Miocene. South-directed thrusting in this transitional area, combined with dextral strike slip reactivating Dinaric structures, is still seismically active (e.g. Kastelic et al., 2008; see yellow line marking the presently active plate boundary in the Alps in Fig. 1).

An east- to northeast-dipping positive V_p anomaly is partly imaged beneath the Dinarides in profile 16 (Fig. 5c) but is lacking in profile 11 (Fig. 6b), which crosses the Dinaric Front to the south. Though the resolution in this latter profile is very poor, the lack of a discernable slab is consistent with previous teleseismic studies (e.g. Bijwaard and Spakmann, 2000; Wortel and Spakmann, 2000; Piromallo and Morelli, 2003; Spakman and Wortel, 2004; Serretti and Morelli, 2011; Koulakov et al., 2009), which support the idea

of a slab gap in the northernmost Dinarides. Ustaszewski et al. (2008), Schefer et al. (2011) and Horvath et al. (2015) invoked asthenospheric upwelling at the SE limit of the Pannonian Basin associated with the break-off of part of the NE-dipping Adriatic slab. This is thought to have permitted asthenosphere to flow from beneath the Adriatic Plate to below the extending Pannonian Basin in the upper plate of the retreating Carpathian subduction (Jolivet et al., 2009; Handy et al., 2015; Horvath et al., 2015; Kiraly et al., 2018).

5.6 Summary of the tectonic interpretation

We summarize by combining all the profiles in Appendix A as a basis for interpreting horizontal depth slices (Figs. 8, 9). The 240 km depth slice in Fig. 8 maximizes the number of slabs intersected and exhibits various degrees of attachment of the slabs to their orogenic edifice and their forelands. The horizontal depth slice of Fig. 9 at 90 km visualizes areas of negative V_p in the uppermost mantle.

Figure 8 shows that in the Alps, slab attachment is only complete in the central and northern western Alps between 7 and 10° E. This is corroborated by surface wave tomography (Kaestle et al., 2018, their Fig. 12) indicating continuous positive velocity anomalies down to depths below 180 km in the central Alps. Detachment is complete in the southernmost western Alps and modest in the eastern central Alps between 10 and 12°. It is complete in the eastern Alps east of about 12° E where we observe the detached eastern Alps slab (Fig. 8) dipping to the northeast (e.g. Lippitsch et al., 2003; see Fig. 4b, c and 6a). No significant positive V_p anomaly is seen at 240 km depth in the easternmost eastern Alps and the Western Carpathians east of 15° E, where the relics of former slabs reside below the 410 km discontinuity (see Fig. 5). Where detachment is complete, the slabs have been supplanted by upwelling asthenosphere, as is seen by three areas of negative V_p anomalies outlined in the depth slice for 90 km (Fig. 9) in the southern western Alps, the Veneto volcanic province and the Pannonian Basin. In the Apennines, the Adriatic slab is locally hanging but mostly completely detached from its overlying orogenic root and foreland. There, too, upwelling asthenosphere has locally replaced the descending slab in the frontal, i.e. NE, parts of the orogen, eliminating the former connection of the slab with the remaining undeformed part of the Adriatic Plate in the Adriatic Sea.

Figure 9 also features a dashed green line marking the location of the Alpine Tethys suture zone projected from the crust down to 90 km, separating the European lithosphere from the Adriatic lithosphere. We emphasize that the downward projection of this suture in the profiles (dashed green lines) is hypothetical in the sense that mapping it involved tracing the suture through domains that were extensively modified during delamination and mantle upwelling. The severe bending of the putative trace of this suture zone at the Alps–Apennines junction reflects anticlockwise rotation of

the Corsica–Sardinia block and the Ligurian Alps in Miocene times (Schmid et al., 2017, and references therein). Likewise, bending of the projected suture north of the Mid-Hungarian Fault Zone is due to the anticlockwise rotation of the Western Carpathians, also in Neogene times (Márton et al., 2015).

6 Discussion

6.1 Subduction polarity – was there a switch in the Alps?

The polarity of subduction in the Alps, particularly at its junction with the northern Dinarides, has been a bone of contention ever since the publication of P-wave tomographic images showing a high-velocity anomaly some 200 km long dipping some 50° to the northeast beneath the eastern Alps (Babuska et al. 1990) and connected with the upper mantle of the undeformed Adriatic Plate according to Lippitsch et al. (2003). The eastern Alps slab was thought to be separated from the SE-dipping European slab anomaly in the central and western Alps by a decrease in strength of the positive anomaly, interpreted by these authors as a slab gap in map view. The attribution of the eastern Alps slab to the Adriatic Plate by Lippitsch et al. (2003) was challenged by Mitterbauer et al. (2011), whose teleseismic model showed a steeper (75° or more) and longer eastern Alps slab reaching down to the 410 km discontinuity. The eastern Alps slab was thought to have been Adriatic lithosphere that had been laterally wedged from the Dinarides (Lippitsch et al., 2003) or subducted beneath the eastern Alps in Neogene times (Schmid et al., 2004; Kissling et al., 2006; Handy et al., 2015). Although N-directed subduction was inconsistent with north-vergent nappe stacking along strike of the entire Alpine chain, these authors postulated a late-stage switch in subduction polarity in Miocene times, i.e. after nappe stacking. Another possible problem with a Miocene switch in subduction polarity is that the easternmost part of the slab anomaly imaged by Lippitsch et al. (2003) is significantly longer (200 km) than the estimated amount of south-directed shortening in the eastern southern Alps, which amounts to ≥ 50 km (Schönborn, 1999; Nussbaum, 2000). One way to explain the excess slab length was also to take into account some 85 km of Miocene N–S shortening accommodated in the eastern Alps and some 55 km Miocene shortening taken up at the front of the northernmost Dinarides (Ustaszewski et al., 2008, their Fig. 6). Another way was to assume that the eastern part of the slab is partly of European origin (Handy et al., 2015). Indeed, recent models based on pre-AlpArray seismological data have combined ambient noise and P-wave tomography to propose that eastern Alps slab is actually a composite of predominantly European lithosphere and a subordinate amount of Adriatic lithosphere (Kästle et al., 2020).

Our new results clearly show that there is only one slab below the Alps rather than the two proposed by adherents of a switch in subduction polarity. A switch in the polarity of subduction beneath the Alps can thus be ruled out based on our new data. The notion of only one continuous European slab beneath the Alps was previously advanced by Mitterbauer et al. (2011), with the added observation that this slab is overturned and acquires a northward dip in the eastern Alps, as also noted in our profiles (Fig. 4). A comparison of profiles across the eastern Alps between the model of Lippitsch et al. (2003) in Fig. 10a and this work (Fig. 10b) demonstrates the poor fit of the models and highlights why mantle delamination and slab detachment rather than a change in subduction polarity are the most recent processes to leave their imprint in the eastern Alps. The most striking difference, apart from the length of the slab, is that the detached European slab according to our model has no connection to the Adriatic lithosphere from which it is separated by low-velocity upper mantle (Fig. 10b).

The length of the slab measured in profiles varies along strike between 220 and ≥ 500 km, with even the latter estimate regarded as a minimum given that in some profiles the positive anomalies continue below the 410 km discontinuity into the mantle transition zone (e.g. profile 8 in Fig. 3a and profiles 6, 8, A and C in Appendix A). These lengths are not a reliable measure of the amount of subducted lithosphere because the slabs appear to be highly deformed and, anyway, resolution decreases at such depths (Foulger, 2013). Nevertheless, the range of lengths overlaps with palinspastic estimates of the total width of the Alpine Tethyan domain and its continental margins in the Alps subducted between 84 and 35 Ma as measured in a NNW–SSE direction parallel to Adria–Europe convergence (350–400 km, Le Breton et al., 2021; van Hinsbergen et al., 2020; 500 km, Handy et al., 2010). An interesting implication of this overall consistency between subducted and seismically imaged lithosphere is that potentially more of the Alpine subduction is preserved in the mantle than hitherto believed. Based on earlier teleseismic tomography, Handy et al. (2010) estimated a deficit between subducted and imaged lithosphere of between 10 % and 30 %, depending on the contour intervals of positive P-wave anomalies used in their areal assessments of positive anomalies.

The steep northward dip of the part of the European slab beneath the eastern Alps must have been acquired after southward subduction of the European lithosphere stopped in this part of the Alps. The youngest exhumed high-pressure rocks that are testimony to an exhumed subduction zone in this part of the Alps are found in the central Tauern Window (Gross et al., 2000) and the age of subduction-related metamorphism is estimated to be around 35–45 Ma (Kurz et al., 2008; Ratschbacher et al., 2004, and references therein). A younger age range for this metamorphism was proposed (32–35 Ma, allanite U–Pb; Smye et al., 2011; Lu-Hf, Nagel et al., 2013), but these are inconsistent with evidence of substantial exhumation of high-pressure units before the intrusion of the periadriatic plutons and the onset of movements along

the Periadriatic Fault System (Rosenberg, 2004). The 35–45 Ma age range for HP metamorphism certainly pre-dates indentation of the eastern southern Alps along the Giudicarie Belt starting at around 23 Ma (Scharf et al., 2013). Hence, roll-back and steepening of the European slab, followed by slab detachment and rotation of the detached eastern Alps slab into a steeply N-dipping orientation most likely occurred sometime within the 39–23 Ma time interval, most likely at around 23 Ma according to geological evidence (e.g. Scharf et al., 2013). The mechanisms of such rotation and verticalization during the opening of the Pannonian back arc behind the European slab subducting beneath the Eastern Carpathians are unclear. The slab might have been twisted while still attached to a descending slab relict beneath the Pannonian Basin (profile 5 in Fig. 5b; Dando et al., 2011). However, we favour reorientation of the slab by asthenospheric flow during or after northward Adriatic indentation and slab detachment in Neogene times (e.g. Ratschbacher et al., 1991; Favaro et al., 2017). The arcuate convex northward pattern of fast SKS (split shear wave) directions beneath the eastern Alps is suggestive of east-directed asthenospheric flow (e.g. Qorbani et al., 2015) and would be consistent with both of these interpretations.

6.2 Slab attachment and detachment

An intact slab dipping down to a depth of 300 km and beyond is only observed beneath the western to central (Swiss–Italian) Alps between latitudes 7 and 10° E (see area marked as undetached in Fig. 8; profiles 6 and 9 in Appendix A). Interestingly, Singer et al. (2014) noticed that lower crustal seismicity in the European lithosphere is restricted to this same range of latitudes. They proposed that this deep crustal seismicity is driven by stresses transferred to the foreland from the still attached segment of the European slab, which they argue is steepening as it retreats toward the foreland. Kissling and Schlunegger (2018; their Fig. 5c) present a schematic 3D diagram of this remaining undetached European slab, arguing that such slab retreat during attachment is responsible for the striking isostatic disequilibrium between the low surface topography and the thick crustal root (some 50 km, e.g. Spada et al., 2013) beneath this segment of the Alps.

Complete delamination during the advanced stages of detachment of the European lithosphere occurred in the eastern Alps and resulted in a broad zone of low-velocity material interpreted as being upwelling mantle (Fig. 9), typically at a depth between 70 and 130 km (e.g. profile 15 in Fig. 5a) east of 12° E (i.e. east of the western Tauern Window, Fig. 1). East of 15° E, no substantial remnants of the European slab are found above the 410 km discontinuity (Fig. 8 and profiles 5, 11, 10 in Appendix A). This conforms to the findings of Dando et al. (2011) and indicates that roll-back subduction in the Carpathians followed by detachment of the European slab played a fundamental role in forming the greater Pan-

nonian area (Horvath et al., 2006; Matenco and Radivojević, 2012). West of the Tauern Window, between 12° and about 9.5° E, traversed by profile B (Fig. 3c), detachment is only moderate. A third area in the Alps where substantial detachment occurs is the southern part of the western Alps (profiles 8 in Fig. 3a and A in Appendix A) that is transitional to the Northern Apennines. Such detachment was first noticed by Lippitsch et al. (2003; their profile A-A′) but recently refuted by Zhao et al. (2016). There, the detached European slab of the Alps slab resides beneath the westernmost Apennines at a depth of 240 km, while upwelling mantle occupies the area beneath the western Alps at this same depth (Fig. 8).

The completely detached slab beneath most of the Northern Apennines (except for the westernmost parts) hangs subvertically (profiles 11 and 12 in Fig. 6; profile C in Appendix A), confirming the findings of Giacomuzzi et al. (2011, 2012) from teleseismic tomography but at odds with the interpretation of still attached continental slabs without oceanic precursors in Sun et al. (2019). A clear boundary between the European slab under the westernmost Apennines and the delaminated Adriatic mantle lithosphere of the Northern Apennines slab cannot be resolved in the horizontal depth slices but is evident in profiles (e.g. Fig. 3a), where we interpret the boundary between the two slabs to coincide with the Alpine Tethys suture.

6.3 Nature of low-velocity domains in the greater Alpine area

In the text and profiles above, we interpret low-V_p areas within the circum-Adriatic area as resulting from upwelling mantle material (Pannonian Basin, eastern Alps) and hydration effects (Veneto Basin), whereas negative V_p areas in the lower part of the European lithosphere reflect inherited Variscan or pre-Variscan structural anisotropy and/or compositional differences rather than enhanced temperature (Sect. 4).

Insight into the nature of the European lithosphere comes from the striking coincidence of its lower layer of large $-V_p$ anomaly (Figs. 2, 7) with NE–SW-oriented SKS directions and 1–2 s delay times reported for this area in the literature (Barruol et al., 2011) and AlpArray studies (Link and Rümpker, personal communication, 2021). Given a relation of 100 km thickness for every second of delay time, one obtains a thickness of 100–200 km for the anisotropic layer, which matches the observed thickness of the $-V_p$ layer. A well-known effect of azimuthal anisotropy is to retard near-vertically incident body waves (Hammond, 2014; Munzerová et al., 2018), thus providing a possible explanation for the anomalous $-V_p$ layer. Taken together, this suggests that the $-V_p$ layer in the lower European lithosphere is structurally anisotropic and may have accommodated viscous flow. This is contrary to previous interpretations in which the anisotropy was attributed to arc-parallel asthenospheric flow around the European slab (Barruol et al., 2011). The NE–

SW orientation of SKS directions below the central Alps is inconsistent with the SE-subduction direction of European lithosphere, leaving a Variscan or pre-Variscan age for lower-lithospheric flow as the most likely alternative.

We regard a thermal anomaly as unlikely to have caused the large $-V_p$ anomaly in the European lithosphere because the ΔT-values corresponding to the observed $5\% - 6\% -V_p$ would be unrealistically high (300–600°C using the ΔV_p–T relations of Goes et al., 2000; Cammarano et al., 2003; Perry et al., 2006) for old, inactive mantle lithosphere in the down-going plate of a collisional orogen. Variscan crust in the foreland of the Alps underwent amphibolite- to locally granulite-facies regional metamorphism some 340–360 Myr ago, followed by calc-alkaline magmatism and thermal over-printing at 320–260 Ma (e.g. Matte 1986; Franke, 2000, and references therein). This late Carboniferous to early Permian magmatic event is at least 200 Myr older than the onset of collision in the Alps at 40–32 Ma (e.g. Handy et al., 2010, and references therein). Though it has been argued that compositional differences can stabilize vertical and horizontal thermal gradients (Jordan, 1975, 1981), thus contributing to the longevity of the observed seismic heterogeneity, there is no known mechanism to maintain such a pronounced thermal anomaly for such a long time.

Regarding the Adriatic Plate, the question remains of whether the younger, low-V_p patches attributed to Miocene asthenospheric upwelling following lithospheric delamination (Fig. 9) still represent volumes of substantially elevated temperatures today. In view of the fact that water content in addition to temperature influences seismic wave velocities in the mantle (Karato and Jung, 1998; Shito et al., 2006), we propose that at least in the case of the Veneto volcanic province (Fig. 8) temperature is unlikely to be the dominant factor, especially given that present-day heat flow in the Adriatic region is low (Giacomuzzi et al., 2011).

6.4 Timing of slab detachment and its geodynamic consequences

A rough estimate of the time since slab detachment in the eastern Alps can be obtained from the average sink rate of slabs around the world (12 mm/a, van der Meer et al., 2010, 2018). The rate is derived from a compilation of teleseismically imaged slabs of known lengths and ages that are still attached to their lower plate lithospheres, mostly in circum-Pacific convergent zones. When applied to the eastern Alps, this approach yields minimum values of the time since detachment because delamination of the European lithosphere is inferred to have preceded slab detachment (Figs. 4 and 6). They range from 10 to 25 Myr, respectively, beneath the eastern Alps and the Pannonian Basin. The 10–25 Myr time range since slab detachment encompasses the period of orogen-parallel extension and rapid exhumation and lateral escape in the Tauern Window (23–11 Ma, e.g. Scharf et al., 2013) and overlaps with the duration of extension in the Pannonian Basin (21–15 Ma, Horvath et al., 2015, and references therein). This supports our suggestion that lithospheric delamination, slab detachment and asthenospheric upwelling were instrumental in triggering decoupling that enabled Neogene orogen-parallel lateral extrusion of the AL-CAPA tectonic mega-unit (upper-plate crustal edifice of the Alps and Carpathians) towards the Pannonian Basin. This raises questions about the depth of detachment at the base of the ALCAPA mega-unit during its lateral extrusion and the nature of the Moho beneath the Pannonian Basin. Horvath et al. (2015) proposed that during lateral extrusion the extending crust of the ALCAPA mega-unit directly overlay the hot asthenosphere of the Carpathian embayment, and that since then, most of the Pannonian Basin had cooled, allowing a new mantle lithosphere to accrete. If correct, this would imply that the Moho imaged beneath the Pannonian Basin is of Miocene or younger age.

An intriguing aspect of Adriatic indentation and Alpine slab detachment is their potential effects on the foreland and hinterland basins of the Alps. The 25–10 Ma time window for slab detachment brackets the time when thrusting in the eastern Molasse Basin stopped advancing (21–22 Ma) and changed from in-sequence to out-of-sequence (wedge-top) mode (Hinsch, 2013). It also includes the time when the basin rapidly filled with terrigenous components at 19–18 Ma (Grunert et al., 2013), leading to a shift in the paleo-drainage direction from eastward to northwestward (Kuhlemann and Kempf, 2002). Subsequent uplift and erosion of the entire Molasse Basin at 10 to 5 Ma (Cederbom et al., 2011) was greater in the east (0.3–0.5 km) than the west (0.5–1.5 km, Baran et al., 2014). These first-order orogen-parallel variations in foreland basin fill and erosion may be related to the degree of slab attachment, with full attachment in the central Alps lengthening the flexural response of the foreland to slab loading, whereas complete slab detachment and delamination in the east after 25–20 Ma (Handy et al., 2015) favoured a very rapid decrease in basin depth (Genser et al., 2007). This period at 23 Ma coincided with the aforementioned onset of rapid exhumation in the Tauern Window (Fügenschuh et al., 1997) and eastward escape of the eastern Alps into the Pannonian Basin in the upper plate of the retreating Carpathians (Ratschbacher et al., 1991; Scharf et al., 2013).

Finally, a rather vexing consequence of the calculations above is that the 25–10 Ma time window for slab detachment is younger than the 43–29 Ma age range of collision-related intrusives along the Periadriatic Fault (e.g. Müntener et al., 2021). We note that these calc-alkaline intrusives reach from the western Alps to the eastern end of the Alps bordering the Pannonian Basin (Fig. 1). This lateral extent (7.5–16° E, Fig. 1) is much wider than the narrow corridor of slab attachment between 7–10° E in the central Alps (Fig. 8), suggesting that detachment of slab segments along the Alpine chain may have had little, if anything, to do with periadriatic magmatism. Thus, either our estimates of slab detachment times above are based on questionable assumptions and the time

since detachment exceeded 25 Myr, or there was an older late Oligocene break-off event involving an originally longer slab than presently imaged.

A further possibility is that the calc-alkaline magmatism with a lithospheric mantle component reflects deep-seated processes other than slab break-off, e.g. volatile fluxing of the Alpine mantle wedge during the final stages of continental subduction (Müntener et al., 2021). This is in line with petrological–geochemical considerations that the temperature during melting was far lower than would be expected for slab break-off or slab edge effects (Müntener et al., 2021).

7 Conclusions

The images presented here resolve some long-standing debates while compelling us to reassess the role of plates and their structure in mountain building. Figure 11 is a graphic attempt to visualize the complex 3D geometry of mantle structure in the area covered by AlpArray. This figure is a composite view of the Alps seen from the southeast, i.e. from a vantage point above the Dinarides, with the Adriatic Plate removed to reveal the slabs. The slabs and foreland structures were constructed from the interpreted outlines in the 19 profiles in Appendix A.

A prime outcome of this study is that the European and Adriatic Plates involved in Alpine collision have first-order differences in seismic structure: the down-going European lithosphere is thick (ca. 180 km) and marked by laterally continuous positive and negative P-wave anomalies. These are believed to be inherited Variscan or pre-Variscan anisotropic and compositional differences. In the central (Swiss–Italian) Alps, they descend as part of a coherent slab from the Alpine foreland to beneath the Northern Alpine Front. In contrast, the Adriatic Plate is thinner (100–120 km) and has a poorly defined base at the lower boundary of $+V_p$ anomalies. The underlying negative anomaly in the depth interval of 120–270 km is attributable partly to compositional effects (e.g. mantle hydration due to upwelling fluids from the Alpine slab) and partly to upwelling asthenosphere in the aftermath of delamination and slab detachment in the Alps and Apennines.

This fundamental difference in the structure of the lower and upper plates may be responsible for two of the most striking features of the Alps compared to other Alpine–Mediterranean orogens, namely the rugged, high-altitude Alpine topography and the disproportionately large amount of accreted, deeply subducted and exhumed lower-plate units exposed in the deeply eroded core of the Alps (Fig. 11). Thick lithosphere is expected to be relatively stiff and buoyant upon entering collision, favouring tectonic underplating of accreted and subducted tectonic units as subduction proceeds. By comparison, "normal" lithosphere, as found in the Adriatic Plate and its slab beneath the Apennines, is expected to sink more easily under its own weight, favouring roll-back

subduction, the development of low topography and upper plate extension with only limited exhumation of subducted units.

Another new outcome of this study is the extent of delamination and detachment of slabs in both the Alps and the Apennines. Detachment is complete in the southwesternmost Alps and, on a much larger scale, in the eastern Alps (Fig. 11) and Western Carpathians. There, relicts of European lithosphere hang at various depths, with depth increasing towards the east and even reaching the MTZ beneath the Pannonian Basin. Large-scale upwelling of asthenosphere was the response of the mantle to delamination of the European lithosphere and downward motion of detached slabs since at least 25 Ma. The asthenosphere below delaminated lithosphere occupies very shallow depths, in some cases immediately below the Moho marking the base of thinned Alpine orogenic crust, which was stretched in Neogene times during lateral orogenic escape and upper-plate extension forming the Pannonian Basin.

In this study, we claim to have resolved the debate over the polarity of Alpine subduction beneath the eastern Alps in favour of a model with a single European slab that originally subducted to the south. The presently steep, northward dip of the now fragmented and deformed eastern Alps slab segment (Fig. 11), which gave rise to the alternative view of northward Adriatic subduction in the first place, is clearly a secondary feature acquired during or after slab detachment.

A lesson learned in collating and interpreting this extraordinary data set has been that, after initially acquiring and processing seismological data, methodological development and tectonic interpretation must go hand in hand if they are to yield meaningful, testable models. Figure 11 is an initial model of tectonic boundaries based on an assessment of geophysical data in a plate kinematic context. The next step is obviously to parameterize this model in order to compare it with independent sources of data and determine its thermomechanical characteristics.

Appendix A: Profiles used in interpretations
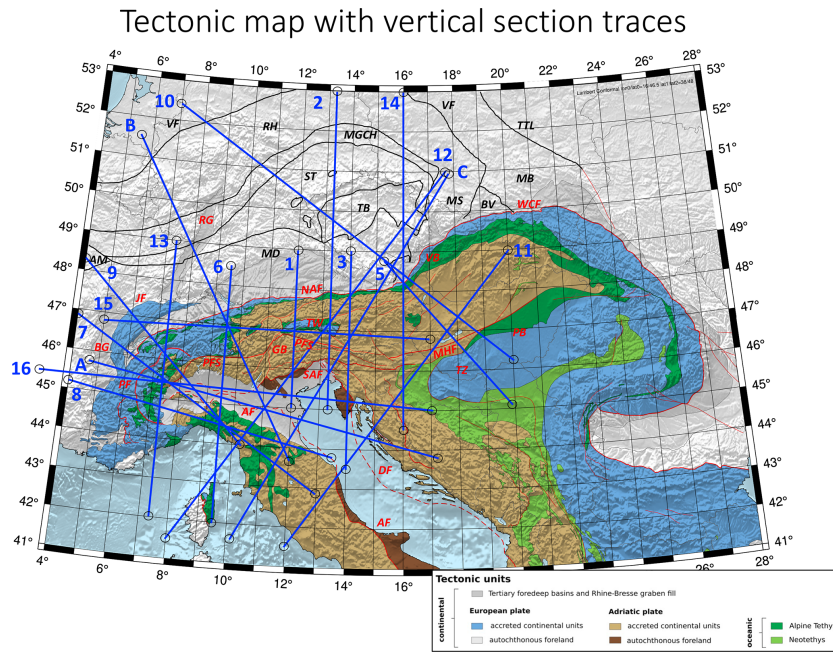
Figure A1. Tectonic map with traces of all tomographic profiles used in this study.
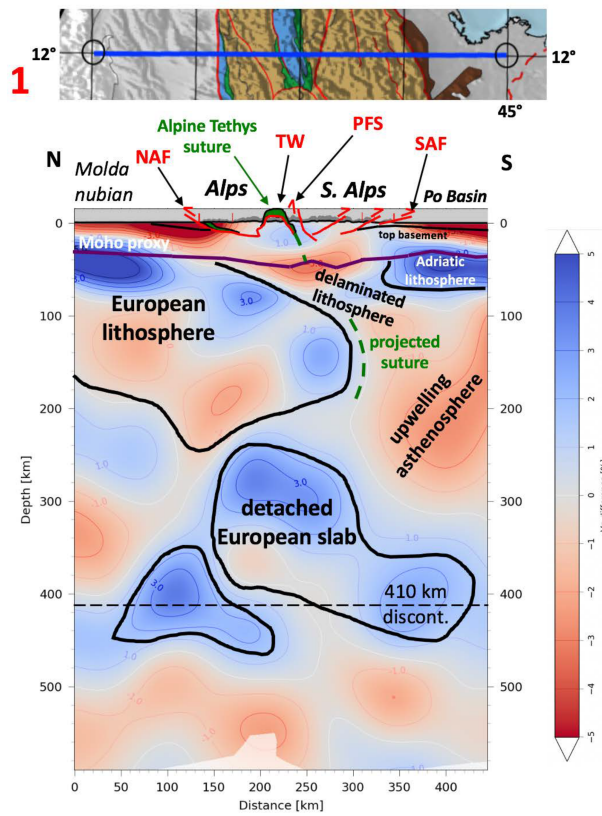
Figure A2. Profile 1.
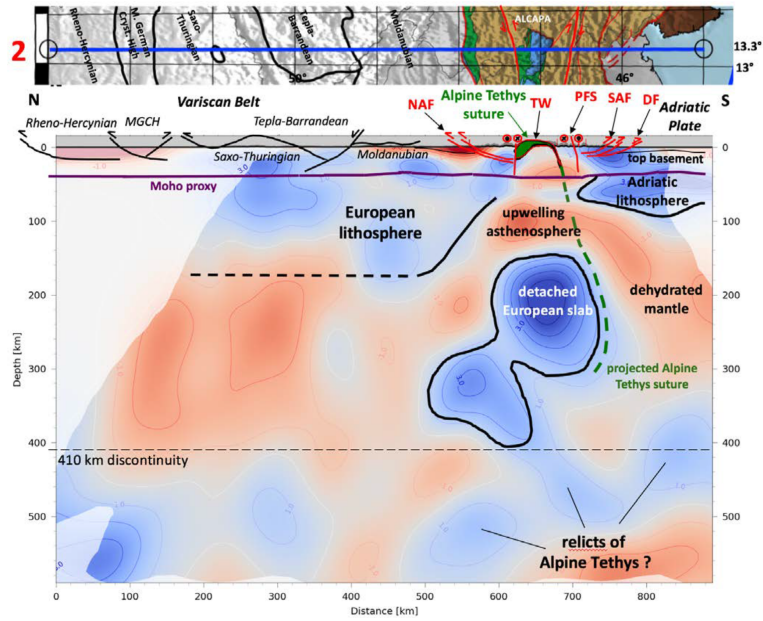
Figure A3. Profile 2.
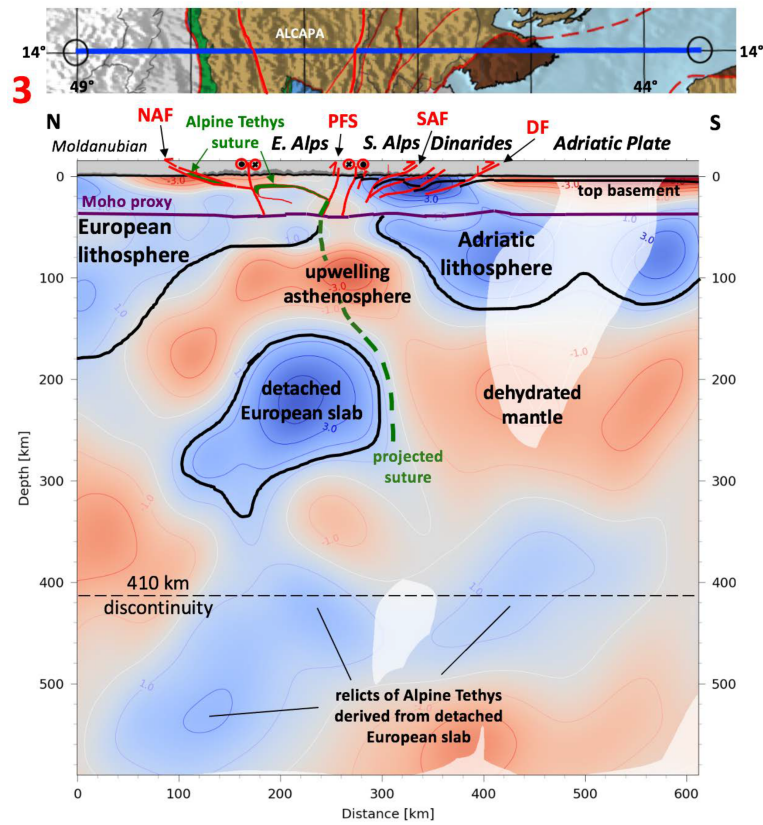
Figure A4. Profile 3.
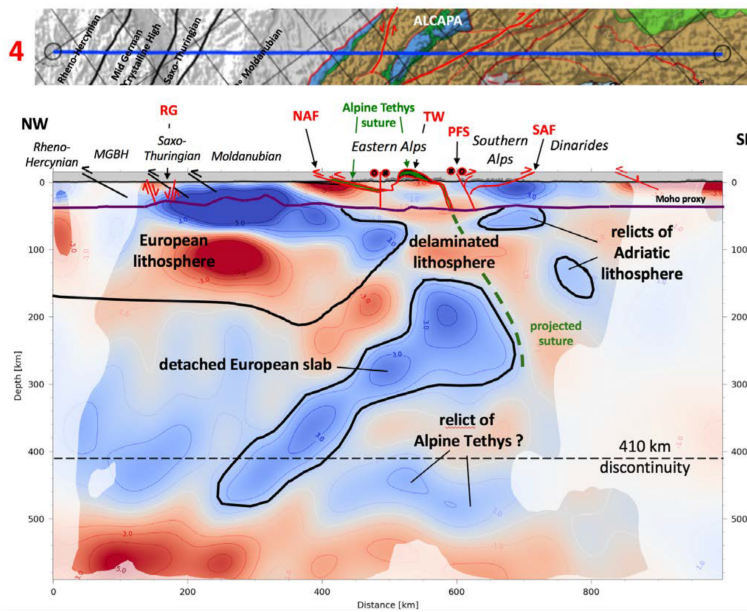
Figure A5. Profile 4.
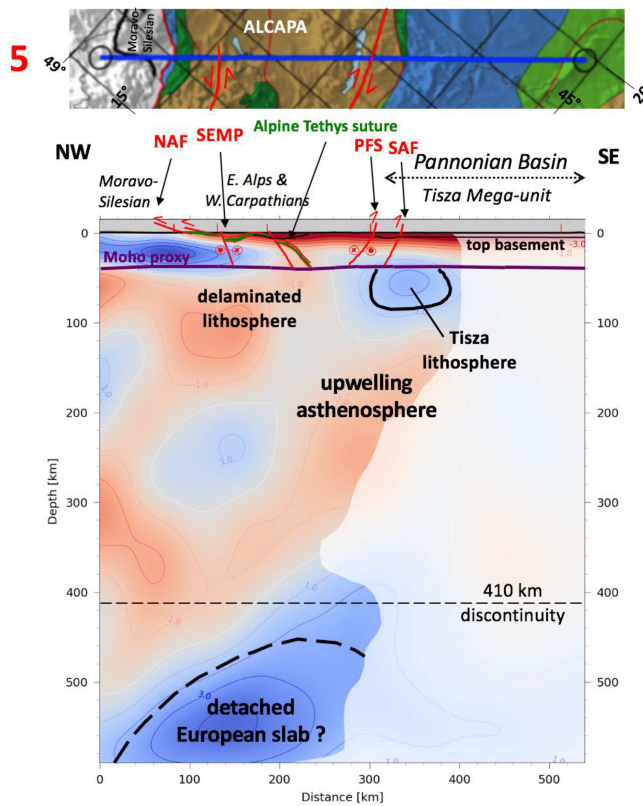
Figure A6. Profile 5.
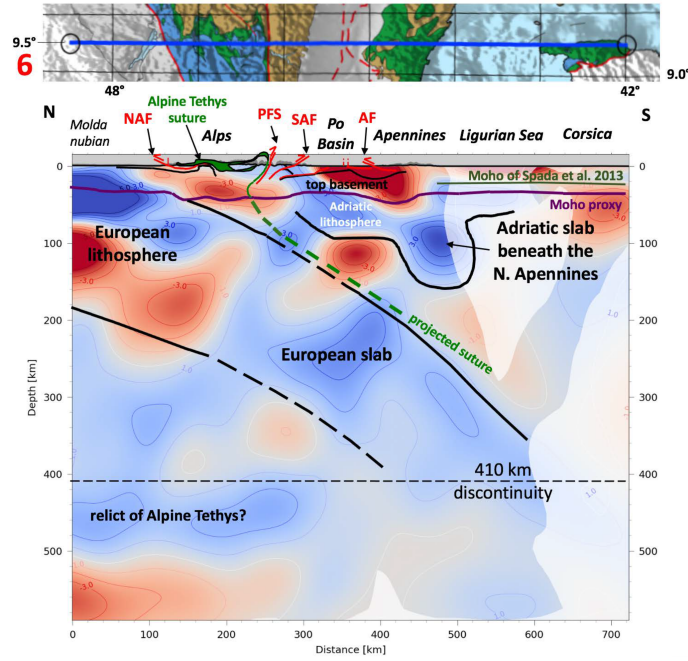
Figure A7. Profile 6.
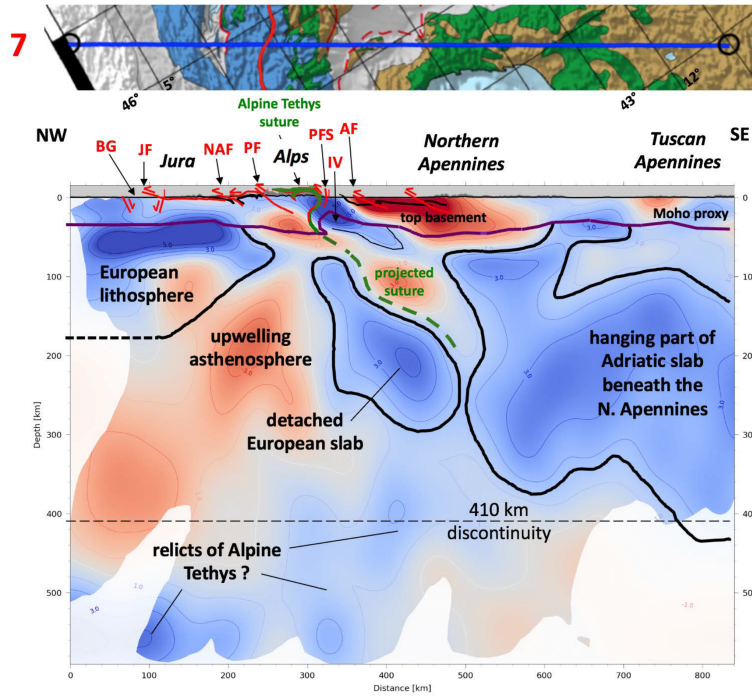
Figure A8. Profile 7.
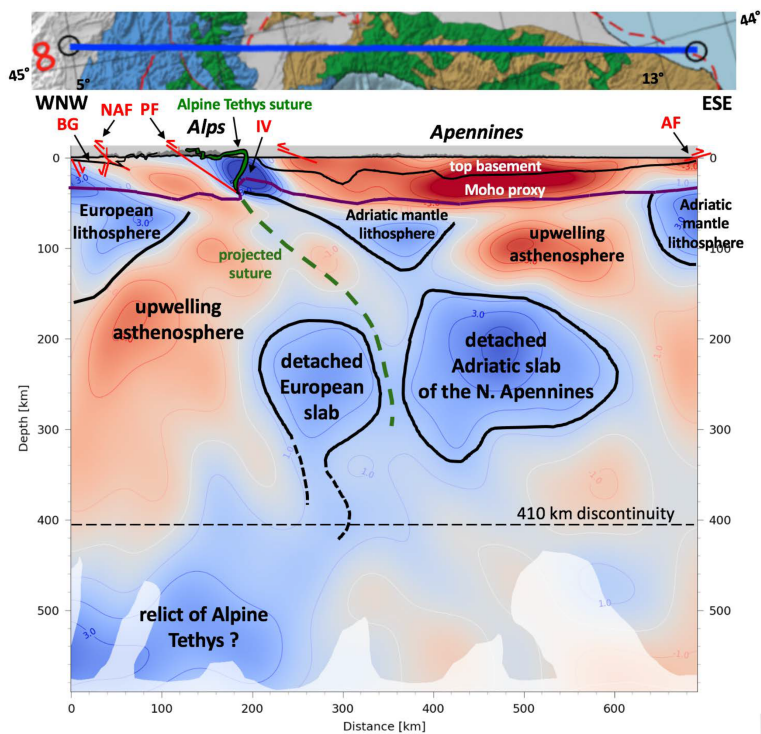
Figure A9. Profile 8.
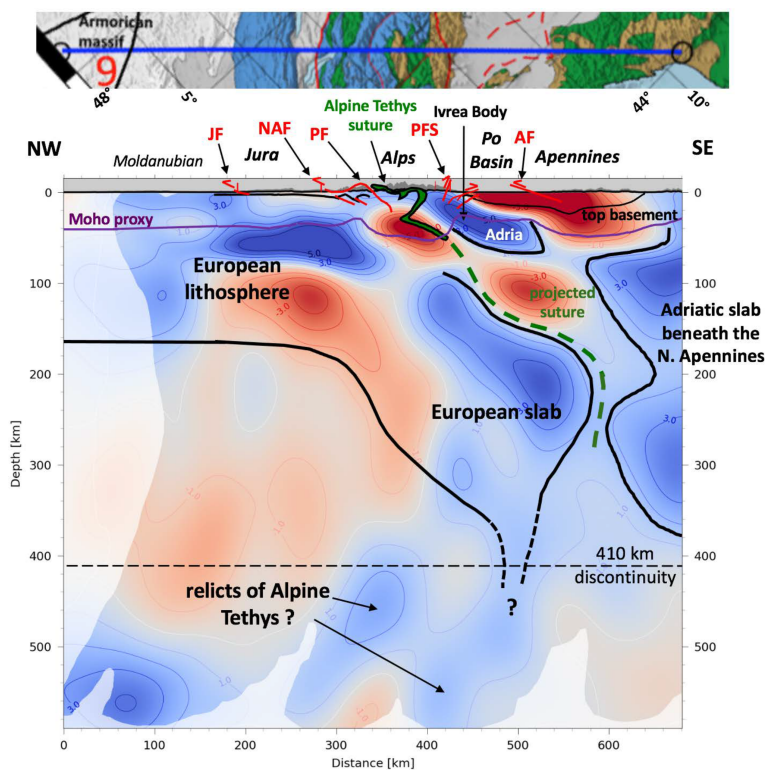
Figure A10. Profile 9.
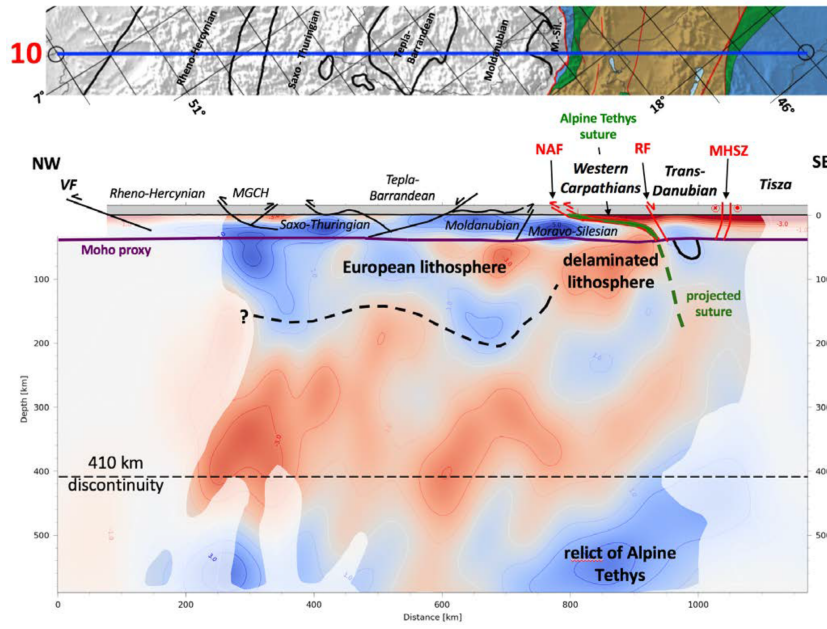
Figure A11. Profile 10.
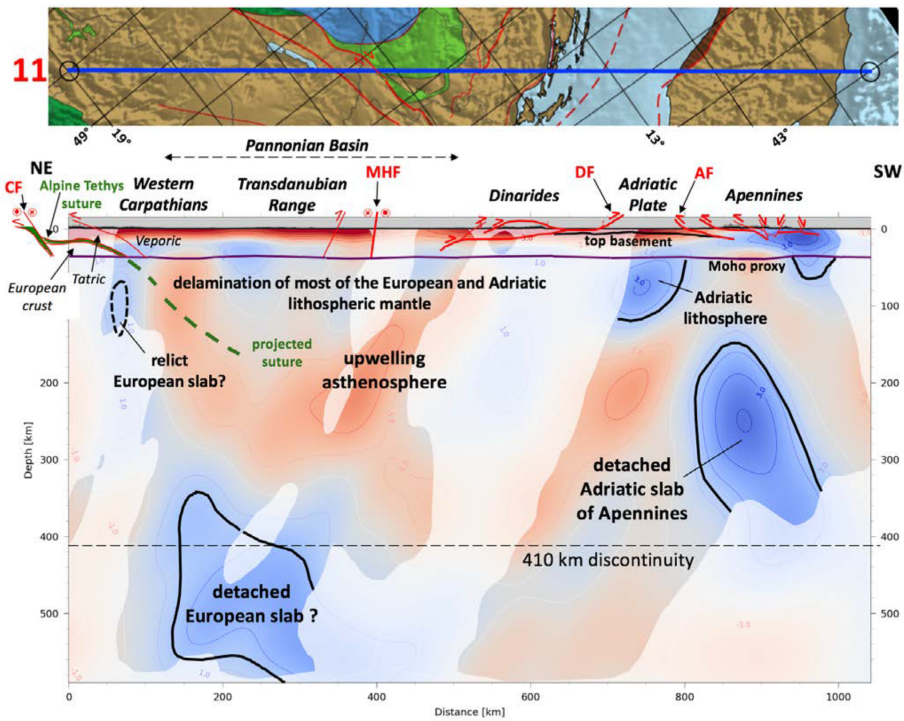
Figure A12. Profile 11.
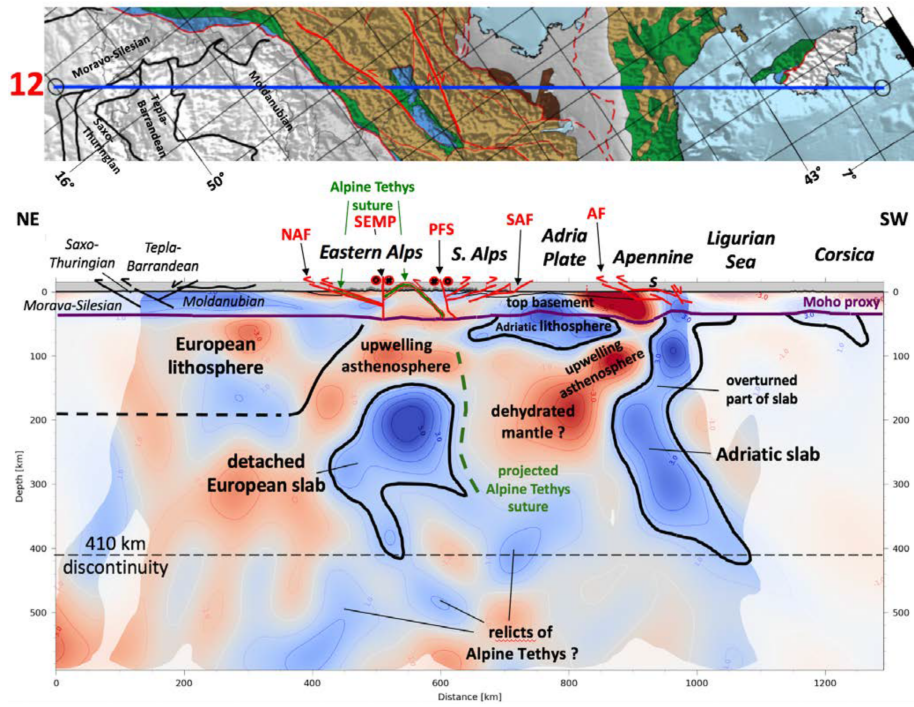
Figure A13. Profile 12.
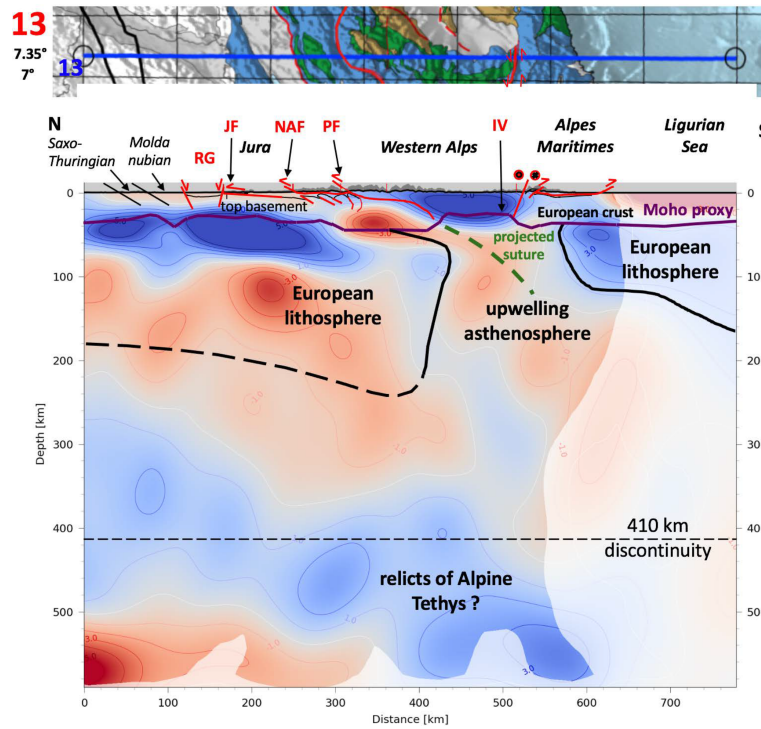
Figure A14. Profile 13.
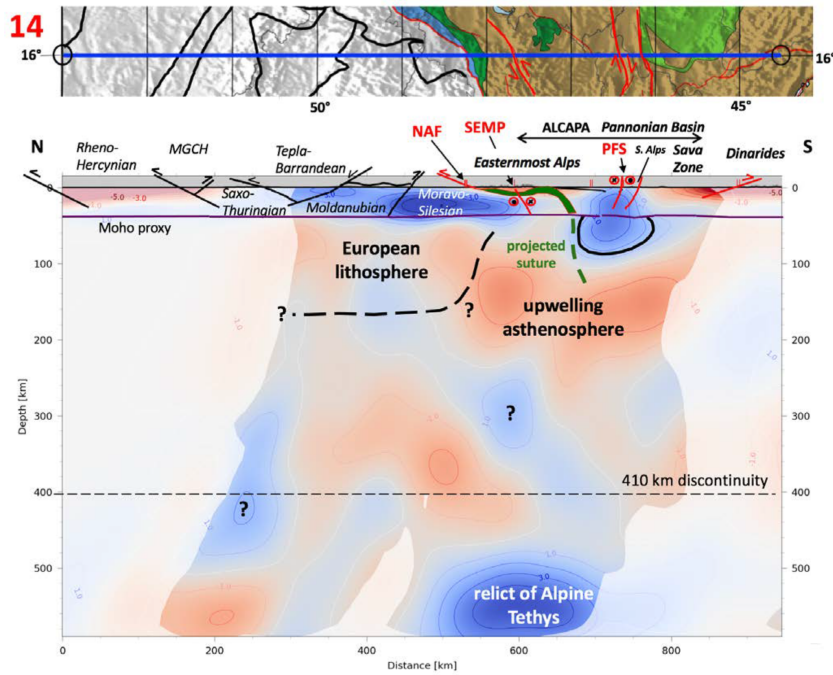
Figure A15. Profile 14.
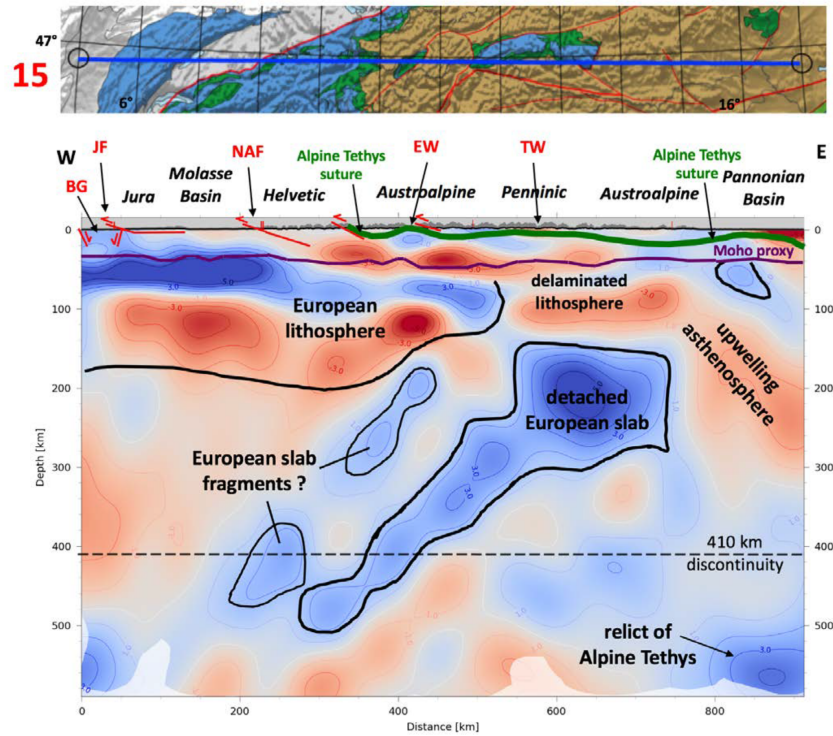
Figure A16. Profile 15.
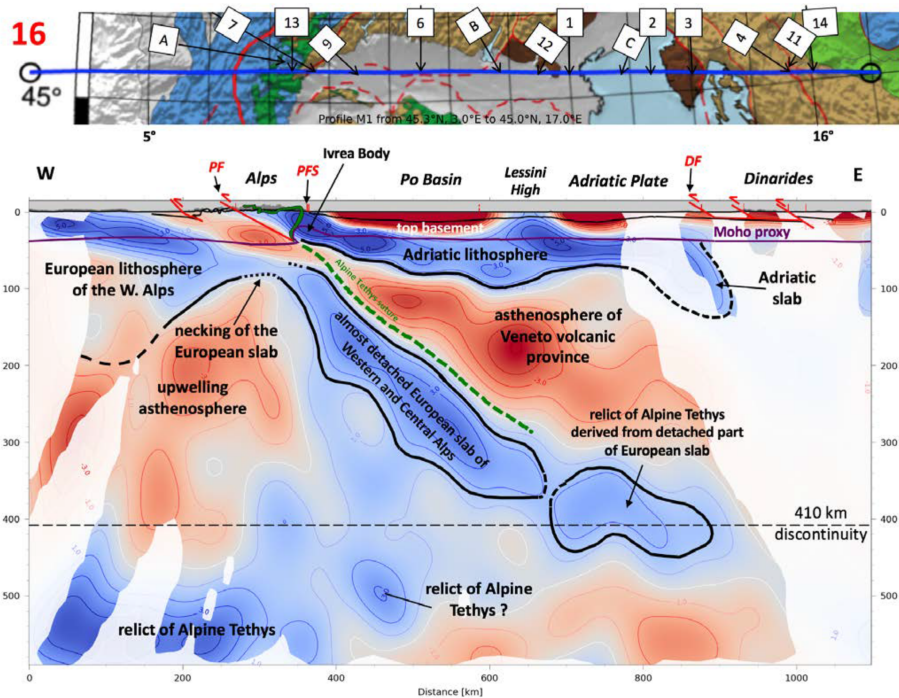
Figure A17. Profile 16. Numbered labels at top indicate intersecting profiles.
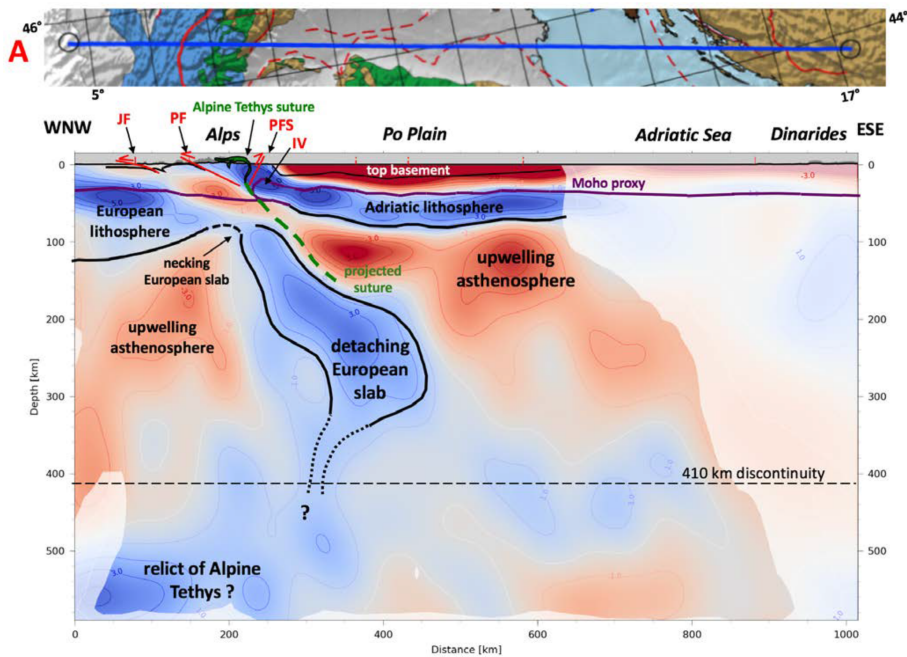
Figure A18. Profile A.
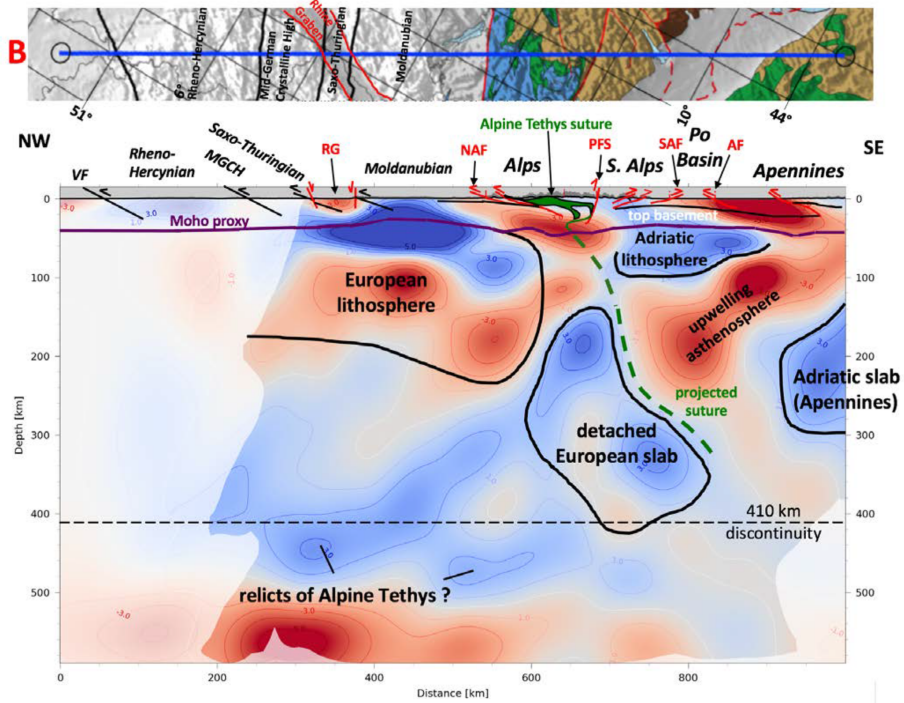
Figure A19. Profile B.
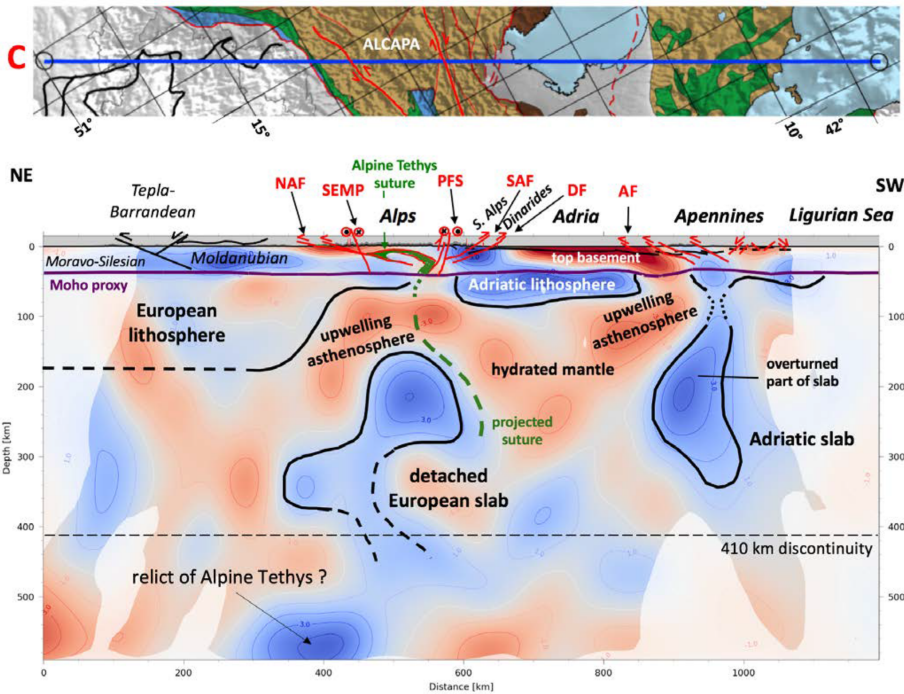
Figure A20. Profile C.

Appendix B: Slab dimensions
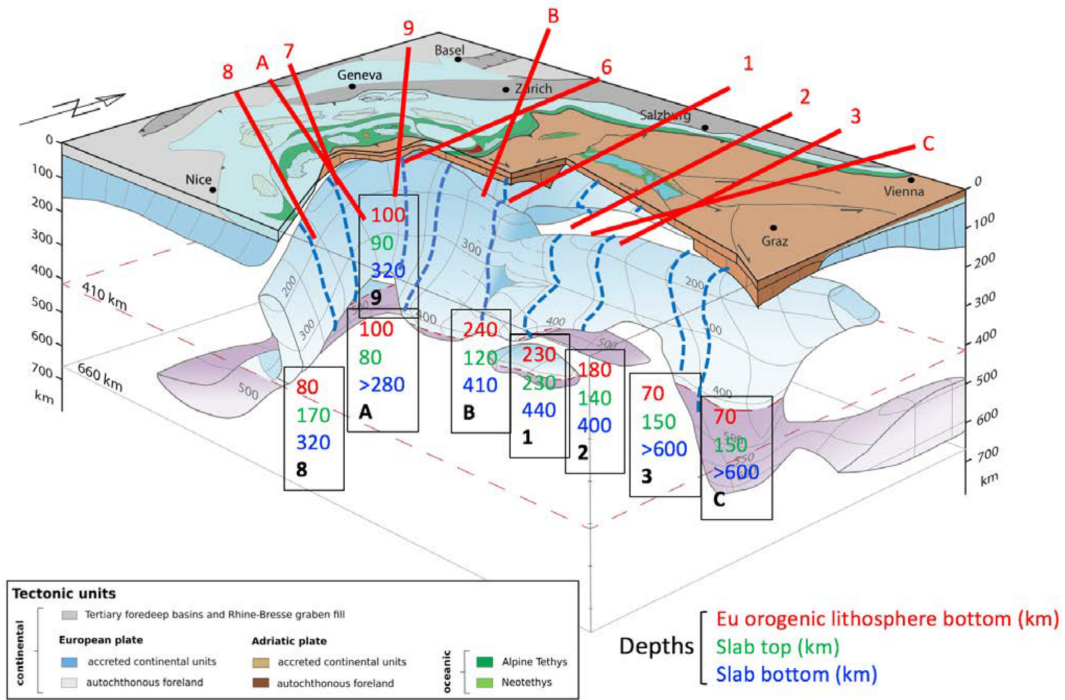
Figure B1. Three-dimensional block diagram with depths to slab tops and bottoms.
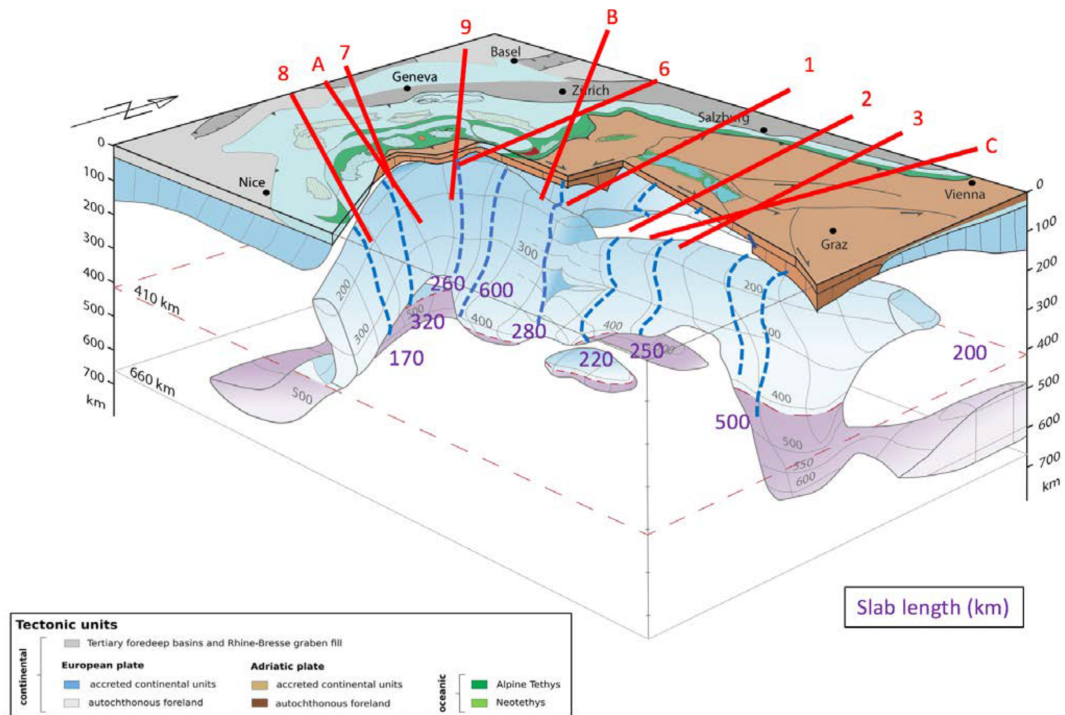
Figure B2. Three-dimensional block diagram with slab lengths.

Author contributions. MH and SS interpreted the tomographic profiles and slices that were provided in raw form by MP. The latter co-author and WF provided the methods that generated the tomographic sections. MH conceived of and wrote the paper with contributions from all co-authors.

Competing interests. The contact author has declared that neither they nor their co-authors have any competing interests.

Special issue statement. This article is part of the special issue "New insights into the tectonic evolution of the Alps and the adjacent orogens". It is not associated with a conference.

Acknowledgements. We acknowledge the generous funding of the German Science Foundation. (DFG) in the form of Special Priority Program 2017 "Mountain-Building in Four-Dimensions (4D-MB). We thank reviewers Stéphane Guillot and Laurent Jolivet as well as the topical editor, Anne Paul, for critical reviews, despite their disagreement with some of our interpretations. Finally, we thank our colleagues in AlpArray for discussions on various topics, some of whom were only marginally involved in this paper but all of whom provided a stimulating background for the ideas presented here: Tobias Diehl, György Hetényi, the late Frank Horvath, Rainer Kind, Edi Kissling, Eline Le Breton, Frederick Link, Thomas Meier, Jan Pleuger, Georg Rümpker, Wim Spakman, Frederik Tilmann, Claudia Piromallo, Othmar Müntener, Phillipe Agard, Anne Bernhardt, Vincent Verwater, Philip Groß and Julian Hülscher. A complete list of members of the AlpArray Working Group can be found here: http://www.alparray.ethz.ch/en/seismic_network/backbone/data-policy-and-citation/.

Financial support. This research has been supported by the Deutsche Forschungsgemeinschaft (DFG) (grant no. Ha-2403/22-1, 23-1, 24-1 and FR-1146/12-1).

We acknowledge support from the Open Access Publication Initiative of Freie Universität Berlin.

Review statement. This paper was edited by Anne Paul and reviewed by Stéphane Guillot and Laurent Jolivet.

References

Agard, P. and Handy, M. R.: Ocean subduction dynamics in the Alps, in: Shedding Light on the European Alps, edited by: Mc-Carthy, A. and Müntener, O., Guest Editors, Elements, 17, 9–16, https://doi.org/10.2138/gselements.17.1.9, 2021.

Argand, E.: Des Alpes et de l'Afrique: Bulletin de la Société Vaudoise des Sciences Naturelles, 55, 233–236, 1924.

Artemieva, I.: The Lithosphere: An Interdisciplinary Approach, Cambridge University Press Monograph, 794 pp., ISBN 9780521843966, 2011.

Babuska, V., Plomerova, J., and Granet, M.: The deep lithosphere in the Alps: a model inferred from P residuals, Tectonophysics, 176, 137–165, https://doi.org/10.1016/0040-1951(90)90263-8, 1990.

Baran, R., Friedrich, A. M., and Schlunegger, F.: The late Miocene to Holocene erosion pattern of the Alpine foreland basin reflects Eurasian slab unloading beneath the western Alps rather than global climate change, Lithosphere, 6, 124–131, https://doi.org/10.1130/L307.1, 2014.

Beccaluva, L., Bianchini, G., Bonadiman, C., Coltorti, M., Milani, L., Salvini, L., Siena, F., and Tassinari, R.: Intraplate lithospheric and sublithospheric components in the Adriatic domain: Nephelinite to tholeiite magma generation in the Paleogene Veneto volcanic province, southern Alps, Geological Society of America Special Paper, 418, 131–152, https://doi.org/10.1130/2007.2418(07), 2007.

Behm, M., Brückl, E., Chwatal, W., and Thybo, H.: Application of stacking and inversion techniques to three-dimensional wide-angle reflection and refraction data of the Eastern Alps, Geophys. J. Int. 170, 275–298, doi.org/10.1111/j.1365-246X.2007.03393.x, 2007

Bigi, G., Castellarin, A., Catalano, R., Coli, M., Cosentino, D., Dal Piaz, G.V., Lentini, F., Parotto, M., Patacca, E., Praturlon, A., Salvini, F., Sartori, R., Scandone, P., and Vai, G.: Synthetic structural kinematic map of Italy, Sheets 1 and 2, C.N.R., Progetto Finalizzato Geodinamica, SELCA Firenze, 1989.

Bijwaard, H. and Spakman, W.: Non-linear global P-wave tomography by iterated linearized inversion, Geophys. J. Int., 141, 71–82, doi:10.1046/j.1365-246X.2000.00053.x, 2000.

Brenker, F. E. and Brey, G. P.: Reconstruction of the exhumation path of the Alpe Arami garnet-peridotite from depths exceeding 160 km, J. Metamorphic Geol., 15, 581–592, doi/abs/10.1111/j.1525-1314.1997.tb00637.x, 1997.

Brückl, E., Bleibinhaus, F., Gosar, A., Grad M., Guterch, A., Hrubcová, P.G., Keller, R., Majdanski, M., Sumanovac, F., Tiira, T., Yliniemi, J., Hegedus, E., and Thybo, H.: Crustal structure due to collisional and escape tectonics in the Eastern Alps region based on profiles Alp01 and Alp02 from the ALP 2002 seismic experiment, J. Geophys. Res., 112, B06308, https://doi.org/10.1029/2006JB004687, 2007.

Cammarano, F., Goes, S., Vacher, P., and Giardini, D.: Inferring upper-mantle temperatures from seismic velocities, Physics of the Earth and Planetary Interiors, 138, 197–222, https://doi.org/10.1016/S0031-9201(03)00156-0, 2003.

Cassano, E., Anelli, L., Fichera, R., and Cappelli, V: Pianura Padana: Interpretazione integrate di dati Geofisici e geologici, 73° Congresso Società Geologica Italiana, Roma, AGIP, 27 pp, 1986.

Champagnac, J. D., Molnar, P., Anderson, R. S., Sue, C., and Delacou, B.: Quaternary erosion-induced isostatic rebound in the western Alps, Geology, 35, 195–198, https://doi.org/10.1130/G23053A.1, 2007.

Chopin, C.: Coesite and pure pyrope in high-grade blueschists of the Western Alps: a first record and some con-

sequences, Contr. Mineral. and Petrol., 86, 107–118, https://doi.org/10.1007/BF00381838, 1984.

Cederbom, C. E., van der Beek, P., Schlunegger, F., Sinclair, H. D., and Oncken, O.: Rapid extensive erosion of the North Alpine foreland basin at 5-4 Ma, Basin Research, 23, 528–550, https://doi.org/10.1111/j.1365-2117.2011.00501.x, 2011.

Dando, B. D. E., Stuart, G. W., Houseman, G. A., Hegedüs, E., Brückl, E., and Radovanovic, S.: Teleseismic tomography of the mantle in the Carpathian–Pannonian region of central Europe, Geophys. J. Int., 186, 11–31, https://doi.org/10.1111/j.1365246X.2011.04998.x, 2011.

Diehl, T., Husen, S., Kissling, E., and Deichmann, N.: High-resolution 3-D P-wave model of the Alpine crust, Geophys. J. Int., 179, 1133–1147, https://doi.org/10.1111/j.1365246X.2009.04331.x, 2009.

Faccenna, C., Piromallo, C., Crespo-Blanc, A., Jolivet, L., and Rossetti, F.: Lateral slab deformation and the origin of the western Mediterranean arcs, Tectonics, 23, TC1012, https://doi.org/10.1029/2002TC001488, 2004.

Favaro S., Handy, M. R., Scharf, A., and Schuster, R.: Changing patterns of exhumation and denudation in front of an advancing crustal indenter, Tauern Window (Eastern Alps), Tectonics, 36, 1053–1071, https://doi.org/10.1002/2016TC004448, 2017.

Foulger, G. R., Panza, G. F., Artemieva, I. M., Bastow, I. D., Cammarano, F., Evans, J. R., Hamilton, W. B., Julian, B. R., Lustrino, M., Thybo, H., and Yanovskaya, T. B.: Caveats on tomographic images, Terra Nova, 25, 259–281, https://doi.org/10.1111/ter.12041, 2013.

Fox, M., Herman, F., Kissling, E., and Willet, S. D.: Rapid exhumation in the Western Alps driven by slab detachment and glacial erosion, Geology, 43, 5, 379–382 https://doi.org/10.1130/G36411.1, 2015.

Fox, M., Herman F., Willett, S. D., and Schmid, S. M.: The exhumation history of the European Alps inferred from linear inversion of thermochronometric data, American Journal of Science, 316, 505–541, https://doi.org/10.2475/06.2016.01, 2016.

Franke, W.: The Mid-European segment of the Variscides: tectonostratigraphic units, terrane boundaries and plate tectonics evolution, Geological Society, London, Special Publications, 179, 35–61, https://doi.org/10.1144/GSL, 2000.

Franke, W., Cock, L. R. M., and Torsvik, T. H.: The Palaeozoic Variscan oceans revisited, Gondwana Research, 48, 257–284, https://doi.org/10.1016/j.gr.2017.03.005, 2017.

Fügenschuh, B., Seward, D., and Mancktelow, N. S.: Exhumation in a convergent orogen: the western Tauern Window, Terra Nova, 9, 213–217, https://doi.org/10.1111/j.1365-3121.1997.tb00015.x, 1997

Geissler, W. H., Sodoudi, F., and Kind, R.: Thickness of the central and eastern European lithosphere as seen by S receiver functions, Geophys. J. Int., 181, 604–634, https://doi.org/10.1111/j.1365-246X.2010.04548.x, 2010.

Genser, J., Cloetingh, S. A. L., and Neubauer, F.: Late orogenic rebound and oblique Alpine convergence: New constraints from subsidence analysis of the Austrian Molasse basin, Glob. Planet. Change, 58, 214–223, https://doi.org/10.1016/j.gloplacha.2007.03.010, 2007.

Giacomuzzi, G., Chiarabba, C., and De Gori, P.: Linking the Alps and Apennines subduction systems: New constraints revealed by high-resolution teleseismic tomography, Earth Planet. Sc. Lett., 301, 531–543, https://doi.org/10.1016/j.epsl.2010.11.033, 2011.

Giacomuzzi, G., Civalleri, M., DeGori, P., and Chiarabba, C.: A 3D Vs model of the upper mantle beneath Italy: Insight on the geodynamics of central Mediterranean, Earth Planet. Sc. Lett., 335, 105–120, doi.org/10.1016/j.epsl.2012.05.004, 2012.

Goes, S., Govers, R., and Vacher, P.: Shallow mantle temperatures under Europe from P and S wave tomography, J. Geophys. Res., 105, 11153–11169, doi.org/10.1029/1999JB900300, 2000.

Grad, M., Tiira, T., and ESC Working Group: The Moho depth map of the European Plate, Geophys. J. Int., 176, 279–292, https://doi.org/10.1111/j.1365-246X.2008.03919.x, 2009.

Grenerczy, G., Sella, G., Stein, S., and Kenyeres, A.: Tectonic implications of the GPS velocity field in the northern Adriatic region, Geophs. Res. Lett., 32, L16311, https://doi.org/10.1029/2005GL022947, 2005.

Gross, P., Handy, M. R., John, T., Pestal, G., and Pleuger, J.: Crustalscale sheath folding at HP conditions in an exhumed Alpine subduction zone (Tauern Window, Eastern Alps), Tectonics, 39, 1–22, https://doi.org/10.1029/2019TC005942, 2020.

Grunert, P., Hinsch, R., Sachsenhofer, R. F., Bechtel, A., Ćorić, S., Harzhauser, M., Piller, W.E., and Sperl, H.: Early Burdigalian infill of the Puchkirchen Trough (North Alpine Foreland Basin, Central Paratethys): Facies development and sequence stratigraphy, Mar. Petrol. Geol., 39, 164–186, https://doi.org/10.1016/j.marpetgeo.2012.08.009, 2013.

Hammond, J. O. S.: Constraining melt geometries beneath the Afar Depression, Ethiopia from teleseismic receiver functions: The anisotropic H-κ stacking technique, Geochem. Geophys. Geosyst., 15, 1316–1332, https://doi.org/10.1002/2013GC005186, 2014

Handy, M. R., Schmid, S. M., Bousquet, R., Kissling, E., and Bernoulli, D.: Reconciling plate-tectonic reconstructions with the geological-geophysical record of spreading and subduction in the Alps, Earth Sci. Rev., 102, 121–158, https://doi.org/10.1016/j.earscirev.2010.06.002, 2010.

Handy, M. R., Ustaszewski, K., and Kissling, E.: Reconstructing the Alps–Carpathians–Dinarides as a key to understanding switches in subduction polarity, slab gaps and surface motion, Int. J. Earth Sci. (Geol. Rundsch.), 104, 1–26, https://doi.org/10.1007/s00531-014-1060-3, 2015.

Hetényi, G. Molinari, I., Clinton, J., Bokelmann, G., Bondár, I., Crawford, W.C., Dessa, J.X., Doubre, C., Friederich, W., Fuchs, F., Giardini, D., Gráczer, Z., Handy, M.R., Herak, M., Jia, Y., Kissling, E., Kopp, H., Korn, M., Margheriti, L., Meier, T., Mucciarelli, M., Paul, A., Pesaresi, D., Piromallo, C., Plenefisch, Th., Plomerová, J., Ritter, J., Ruümpker, G., Šipka, V., Spallarossa, D., Thomas, Ch., Tilmann, F., Wassermann, J., Weber, M., Wéber, Z., Wesztergom, V., Živčić, M., and AlpArray Seismic Network Team , AlpArray OBS Cruise Crew, AlpArray Working Group: The AlpArray Seismic Network: A large-scale European experiment to image the Alpine orogen, Surv. Geophys., 39, 1009–1033, doi.org/10.1007/s10712-018-9472-4, 2018.

Hinsch, R.: Laterally varying structure and kinematics of the Molasse fold and thrust belt of the Central Eastern Alps: Implications for exploration, AAPG Bull., 97, 1805–1831, https://doi.org/10.1306/04081312129, 2013.

Horváth, F., Bada, G., Szafian, P., Tari, G., Adam, A., and Cloetingh, S.: Formation and deformation of the Pannonian Basin: constraints from observational data, in: European Lithosphere Dynamics, edited by: Gee, D. G. and Stephenson, R. A., , Geological Society London Memoirs, 32, 191–206, doi.org/10.1144/GSL.MEM.2006.032.01.11, 2006.

Horváth, F., Musitz, B., Balázs, A., Végh, A., Uhrin, A., Nádor, A., Koroknai, B., Pap, N., Tóth, T., and Wórum, G.: Evolution of the Pannonian basin and its geothermal resources, Geothermics, 53, 328–352, doi.org/10.1016/j.geothermics.2014.07.009, 2015.

Jolivet, L., Faccenna, C., and Piromallo, C.: From mantle to crust: Stretching the Mediterranean, Earth Planet. Sc. Lett., 285, 1–2, 198-209. https://doi.org/10.1016/j.epsl.2009.06.017, 2009.

Jones, A., G., Plomerova, J., Korja, T., Sodoudi, F., and Spakman, W.: Europe from the bottom up: A statistical examination of the central and northern European lithosphere–asthenosphere boundary from comparing seismological and electromagnetic observations, Lithos, 120, 14–29, https://doi.org/10.1016/j.lithos.2010.07.013, 2010.

Jordan, T. H.: The Continental Tectosphere, Rev. Geophys. Space Phys., 13, 3, 1–12, https://doi.org/10.1029/RG013i003p00001, 1975.

Jordan, T. H.: Continents as a chemical boundary layer, Phil. Trans. R. Soc. Lond. A, 301, 359–373, 1981.

Karato, S. and Jung, H.: Water, partial melting and the origin of the seismic low velocity and high attenuation zone in the upper mantle, Earth Planet. Sc. Lett., 157, 193–207, 1998.

Karousová, H., Babuška, V., and Plomerová, J.: Upper-mantle structure beneath the southern Bohemian Massif and its surroundings imaged by high-resolution tomography, Geophys. J. Int., 194, 1203–1215, https://doi.org/10.1093/gji/ggt159, 2013.

Kastelic, V., Vrabec, M., Cunningham, D., and Gosar, A.: Neo-Alpine structural evolution and present-day tectonic activity of the eastern Southern Alps: The case of the Ravne Fault, NW Slovenia, J. Struct. Geol., 30, 963–975, https://doi.org/10.1016/j.jsg.2008.03.009, 2008.

Kästle, E.D., Rosenberg, C., Boschi, L., Bellahsen, N., Meier, T., El-Sharkawy, A.: Slab break-offs in the Alpine subduction zone, Int. J. Earth Sci. (Geol Rundsch), 109, 587–603, https://doi.org/10.1007/s00531-020-01821-z, 2020.

Kind, R., Schmid, S. M., Yuan, X., Heit, B., Meier, T., and the AlpArray and AlpArray-SWATH-D Working Groups: Moho and uppermost mantle structure in the greater Alpine area from S-to-P converted waves, Solid Earth Discuss. [preprint], https://doi.org/10.5194/se-2021-33, in review, 2021.

Király, Á., Faccenna, C., and Funiciello, F.: Subduction zones interaction around the Adria microplate and the origin of the Apenninic arc: Tectonics, 37, 3941–3953, https://doi.org/10.1029/2018TC00521, 2018.

Kissling, E. and Schlunegger, F.: Rollback orogeny model for the evolution of the Swiss Alps, Tectonics, 37, 1097–1115, https://doi.org/10.1002/2017TC004762, 2018.

Kissling, E., Schmid, S. M., Lippitsch, R., Ansorge, J., and Fügenschuh, B.: Lithosphere structure and tectonic evolution of the Alpine arc: new evidence from high-resolution teleseismic tomography, Geological Society of London Memoirs, 32, 129–145, doi.org/10.1144/GSL.MEM.2006.032.01.08, 2006.

Koulakov, I., Kaban, M., Tesauro, M., and Cloetingh, S.: P-and S-velocity anomalies in the upper mantle beneath Europe from to-mographic inversion of ISC data, Geophys. J. Int., 179, 345–366, https://doi.org/10.1111/j.1365-246X.2009.04279.x, 2009.

Kuhlemann, J. and Kempf, O.: Post-Eocene evolution of the North Alpine Foreland Basin and its response to Alpine tectonics, Sedimentary Geology, 152, 45–78, doi.org/10.1016/S0037-0738(01)00285-8, 2002.

Kurz, W., Handler, R., and Bertoldi, C.: Tracing the exhumation of the Eclogite Zone (Tauern Window, Eastern Alps) by 40Ar/39Ar dating of white mica in eclogites, Swiss J. Geosci. 101, Supplement 1, S191–S206, https://doi.org/10.1007/s00015-008-1281-1, 2008.

Le Breton, E., Brune, S., Ustaszewski, K., Zahirovic, S., Seton, M., and Müller, R. D.: Kinematics and extent of the Piemont–Liguria Basin – implications for subduction processes in the Alps, Solid Earth, 12, 885–913, https://doi.org/10.5194/se-12-885-2021, 2021.

Lippitsch, R., Kissling, E., and Ansorge, J.: Upper mantle structure beneath the Alpine orogen from high-resolution teleseismic tomography, J. Geophys. Res., 108, 2376, https://doi.org/10.1029/2002JB002016, 2003.

Lyu, C., Pedersen, H.A., Paul, A., Zhao, L., Solarino, S., and CIFALPS Working Group: Shear wave velocities in the upper mantle of theWestern Alps: new constraints using array analysis of seismic surface waves, Geophys. J. Int., 210, 321–331, https://doi.org/10.1093/gji/ggx166, 2017.

Macera, P., Gasperini, D., Piromallo, C., Blichert-Toft, J., Bosch, D., Del Moro, A., and Martin, S.: Geodynamic implications of deep mantle upwelling in the source of Tertiary volcanics from the Veneto region (South-Eastern Alps), J. Geodynam., 36, 563–590, https://doi.org/10.1016/j.jog.2003.08.004, 2003.

Macera, P., Gasperini, D., Ranalli, G., and Mahatsente, R.: Slab detachment and mantle plume upwelling in subduction zones: an example from the Italian South-Eastern Alps, J. Geodynam., 45, 32–48, https://doi.org/10.1016/j.jog.2007.03.004, 2008.

Maffione, M., Speranza, F., Faccenna, C., Cascella, A., Vignaroli, G., and Sagnotti, L.: A synchronous Alpine and Corsica-Sardinia rotation, J. Geophys. Res., 113, B03104, https://doi.org/10.1029/2007JB005214, 2008.

Malusà, M. G., Frezzotti, M. L., Ferrando, S., Brandmayr, E., Romanelli, F., and Panza, G. F.: Active carbon sequestration in the Alpine mantle wedge and implications for long-term climate trends, Sci. Rep., 8, 1–8, 2018.

Malusà, M. G., Guillot, S., Zhao, L., Paul, A., Solarino, S., Dumont, T., Schwartz, S., Aubert, C., Baccheschi, P., Eva, E., Lu, Y., Lyu, C., Pondrelli, S., Salimbeni, S., Sun, W., and Yuan, H.: The deep structure of the Alps based on the CIFALPS seismic experiment: A synthesis, Geochem. Geophys. Geosys., 22, e2020GC009466. https://doi.org/10.1029/2020GC009466, 2021.

Márton, E., Grabowski, J., Tokarski, A. K., and Túnyi, I.: Palaeomagnetic results from the fold and thrust belt of the Western Carpathians: an overview, Geological Society, London, Special Publications, 425, 7–36, https://doi.org/10.1144/SP425.1, 2015.

Matenco, L. and Radivojević, D.: On the formation and evolution of the Pannonian Basin: Constraints derived from the structure of the junction area between the Carpathians and Dinarides, Tectonics, 31, TC6007, https://doi.org/10.1029/2012TC003206, 2012.

Matte, P.: Tectonics and plate tectonics model for the Variscan belt of Europe, Tectonophysics, 126, 329–332, https://doi.org/10.1016/0040-1951(86)90237-4, 1986.

Mazur, S., Aleksandrowski, P., Gągała, Ł., Krzywiec, P., Żaba, J., Gaidzik, K., and Sikora, R.: Late Palaeozoic strike-slip tectonics versus oroclinal bending at the SW outskirts of Baltica: case of the Variscan belt's eastern end in Poland, Int. J. Earth Sci., 109, 1133–1160, https://doi.org/10.1007/s00531-019-01814-7, 2020.

Mey, J., Scherler, D., Wickert, A. D., Egholm, D. L., Tesauro, M., Schildgen, T. F., and Strecker M. R.: Glacial isostatic uplift of the European Alps, Nat. Commun., 7, 13382, https://doi.org/10.1038/ncomms13382, 2016.

Mitchell, B. J.: Anelastic structure and evolution of the continental crust and upper mantle from seismic surface wave attenuation, Rev. Geophys., 33, 441–462, https://doi.org/10.1029/95RG02074

Mitterbauer, U., Behm, M., Brückl, E., Lippitsch, R., Guterch, A., Keller, G. R., Koslovskaya, E., Rumpfhuber, E. M., and Šumanovac, F.: Shape and origin of the East-Alpine slab constrained by the ALPASS teleseismic model, Tectonophysics 510, 195–206, https://doi.org/10.1016/j.tecto.2011.07.001, 2011.

Molli, G., Crispini, L., Mosca, P., Piana, P., and Federico, L.: Geology of the Western Alps-Northern Apennine junction area: a regional review, Journal of the Virtual Explorer, 36, 1–49, https://doi.org/10.3809/jvirtex.2010.00215, 2010.

Molli, G., Brogi, A., Caggianelli, A., Capezzuoli, E., Liotta, D., Spina, A., and Zibra, I.: Late Palaeozoic tectonics in Central Mediterranean: a reappraisal, Swiss J Geosci, 113, 23, 1-32, https://doi.org/10.1186/s00015-020-00375-1, 2020.

Munzerová, H., Plomerová, J., and Kissling, E.: Novel anisotropic teleseismic body-wave tomography code AniTomo to illuminate heterogeneous anisotropic upper mantle: Part I – Theory and inversion tuning with realistic synthetic data, Geophys. J. Int., 215, 524–545, https://doi.org/10.1093/gji/ggy296, 2018.

Müntener, O., Ulmer, P., and Blundy, J. D.: Superhydrous Arc Magmas in the Alpine Context, Elements, in: Shedding Light on the European Alps, McCarthy, A. and Müntener, O., Guest Editors, Elements, 17, 35–40, https://doi.org/10.2138/gselements.17.1.35, 2021.

Nagel, T. J., Herwartz, D., Rexroth, S., Münker, C., Froitzheim, N., and Kurz, W.: Lu-Hf dating, petrography, and tectonic implications of the youngest Alpine eclogites (Tauern Window, Austria), Lithos, 170, 179–190, https://doi.org/10.1016/j.lithos.2013.02.008, 2013.

Nussbaum, C.: Neogene tectonics and thermal maturity of sediments of the easternmost Southern Alps (Friuli are, Italy), unpublished PhD thesis Université de Neuchâtel, Switzerland, 2000.

Paffrath, M., Friederich, W., and the AlpArray and AlpArray-SWATH D Working Groups: Teleseismic P waves at the AlpArray seismic network: wave fronts, absolute travel times and travel-time residuals, Solid Earth, 12, 1635–1660, https://doi.org/10.5194/se-12-1635-2021, 2021a.

Paffrath, M., Friederich, W., and the AlpArray and AlpArray-Swath D working group: Imaging structure and geometry of slabs in the greater Alpine area – A P-wave traveltime tomography using AlpArray Seismic Network data, Solid Earth Discuss. [preprint], https://doi.org/10.5194/se-2021-58, in review, 2021b. TS1

Perry, H. K. C., Jaupart, C., Mareschal, J.-C., and Shapiro, N. M.: Upper mantle velocity-temperature conversion and composition determined from seismic refraction and heat flow, J. Geophys. Res., 111, B07301, https://doi.org/10.1029/2005JB003921, 2006.

Pfiffner, O. A., Lehner, P., Heitzmann, P., Mueller, St., and Steck, A. (Eds.): Deep Structure of the Swiss Alps: Results of NRP 20: Birkhäuser et al., Basel, 460 pp., ISBN 3-7643 5254 X, 1997.

Pfiffner, O. A. and Hitz, L.: Geologic interpretation of the seismic profiles in the Eastern Traverse (lines E1-E3, E7-E9): eastern Alps, Chapter 9 in Pfiffner et al. (Eds.) Deep Structure of the Alps: Results of NRP 20, Birkhäuser et al., Basel, 73–100, 1997.

Picotti, V. and Pazzaglia, F. J.: A new active tectonic model for the construction of the Northern Apennines mountain front near Bologna (Italy), J. Geophys. Res., 113, B08412, https://doi.org/10.1029/2007JB005307, 2008.

Piromallo, C. and Morelli, A.: P wave tomography of the mantle under the Alpine-Mediterranean area, J. Geophys. Res., 108, 2065, https://doi.org/10.1029/2002JB001757, 2003.

Pomella, H., Klötzli, U., Scholger, R., Stipp, M., and Fügenschuh, B.: The Northern Giudicarie and the Meran-Mauls fault (Alps, Northern Italy) in the light of new paleomagnetic and geochronological data from boudinaged Eo-Oligocene tonalites, Int. J. Earth Sci., 100, 1827–1850, https://doi.org/10.1007/s00531-010-0612-4, 2011.

Pomella, H., Stipp, M., and Fügenschuh, B.: Thermochronological record of thrusting and strike-slip faulting along the Giudicarie fault system (Alps, Northern Italy), Tectonophysics, 79, 118–130, 2012.

Qorbani, E., Bianchi, I., and Bokelmann, G.: Slab detachment under the Eastern Alps seen by seismic anisotropy, Earth Planet. Sc. Lett., 409, 96–108, doi:10.1016/j.epsl.2014.10.049, 2015.

Ratschbacher, L., Frisch, W., Linzer, H.-G., and Merle, O.: Lateral extrusion in the Eastern Alps, part 2: Structural analysis, Tectonics, 10, 257–271 https://doi.org/10.1029/90TC0 2623, 1991.

Ratschbacher, L., Dingeldey, C., Miller, C., Hacker, B. R., and McWilliams, M. O.: Formation, subduction, and exhumation of Penninic oceanic crust in the Eastern Alps: Time constraints from 40 Ar/39 Ar geochronology, Tectonophysics, 394, 155–170, https://doi.org/10.1016/j.tecto.2004.08.003, 2004.

Rawlinson, N. and Sambridge, M.: The Fast Marching Method: An Effective Tool for Tomographic Imaging and Tracking Multiple Phases in Complex Layered Media, Exploration Geophysics, 36, 341–350, https://doi.org/10.1071/EG05341, 2005.

Rawlinson, N., Reading, A. M., and Kennett, B. L. N.: Lithospheric structure of Tasmania from a novel form of teleseismic tomography, J. Geophys. Res., 111, B02301, https://doi.org/10.1029/2005JB003803, 2006.

Rosenberg, C. L.: Shear zones and magma ascent: A model based on a review of the Tertiary magmatism in the Alps, Tectonics, 23, TC3002, https://doi.org/10.1029/2003TC001526, 2004.

Rosenberg, C. L. and Kissling, E.: Three-dimensional insight into Central-Alpine collision: Lower plate or upper-plate indentation?, Geology, 41, 1219–122, https://doi.org/10.1130/G34584.1, 2013.

Rosenberg, C. L., Schneider, S., Scharf, A., Bertrand, A., Hammerschmidt, K., Rabaute, A., and Brun, J.-P.: Relating collisional kinematics to exhumation processes in the Eastern Alps, Earth-Sci. Rev., 176, 311–344, doi.org/10.1016/j.earscirev.2017.10.013, 2018.

Scharf, A., Handy, M. R., Favaro, S., Schmid, S. M., and Bertrand, A.: Modes of orogen-parallel stretching and extensional exhumation in response to microplate indentation and roll-back subduc-

tion (Tauern Window, Eastern Alps), Int. J. Earth Sci., 102, 1627–1654, doi.10.1007/s00531-013-0894-4, 2013.

Schefer, S., Cvetković, V., Fügenschuh, B., Kounov, A., Ovtcharova, M., Schaltegger, U., Schmid, S. M.: Cenozoic granitoids in the Dinarides of southern Serbia: age of intrusion, isotope geochemistry, exhumation history and significance for the geodynamic evolution of the Balkan Peninsula, Int. J. Earth Sci. 100, 1181–1206, https://doi.org/10.1007/s00531-010-0599-x, 2011.

Schertl, H.-P., Schreyer, W., and Chopin, C.: The pyrope-coesite rocks and their country rocks at Parigi, Dora Maira Massif, Western Alps: detailed petrography, mineral chemistry and PT-path, Contrib. Mineral. Petrol., 108, 1–21, 1991.

Schmid, S. M., Pfiffner, O. A., Froitzheim, N., Schönborn, G., and Kissling, E.: Geophysical-geological transect and tectonic evolution of the Swiss-Italian Alps, Tectonics, 15, 1036–1064, doi.10.1029/96TC00433, 1996.

Schmid, S. M., Fügenschuh, B., Kissling, E., and Schuster, R.: Tectonic map and overall architecture of the Alpine orogen, Eclogae Geologicae Helvetiae, 97, 93–117, doi.org/10.1007/s00015-004-1113-x, 2004.

Schmid, S. M., Bernoulli, D., Fügenschuh, B., Matenco, L., Schefer, S., Schuster, R., Tischler, M., and Ustaszewski, K.: The Alpine-Carpathian-Dinaridic orogenic system: correlation and evolution of tectonic units, Swiss J. Geosci., 101, 139–183, https://doi.org/10.1007/s00015-008-1247-3, 2008.

Schmid, S. M., Scharf, A., Handy, M. R., and Rosenberg, C. L.: The Tauern Window (Eastern Alps, Austria): a new tectonic map, with cross-sections and a tectonometamorphic synthesis, Swiss J. Geosci., 106, 1–32, https://doi.org/10.1007/s00015-013-0123-y, 2013.

Schmid, S. M., Kissling, E., Diehl, T., van Hinsbergen D. J. J., and Molli, G.: Ivrea mantle wedge, arc of the Western Alps, and kinematic evolution of the Alps–Apennines orogenic system, Swiss J. Geosci., 110, 581–612, https://doi.org/10.1007/s00015-016-0237-0, 2017.

Schönborn, G.: Alpine tectonics and kinematic models of the central Southern Alps, Mem. Sci. Geol. Padova, 44, 229–393, 1992.

Schönborn, G.: Balancing cross sections with kinematic constraints: The Dolomites (northern Italy), Tectonics 18, 527–545, doi.org/10.1029/1998TC900018, 1999.

Schulmann, K., Lexa, O., Vojtech J., Lardeaux, J. M., and Edel, J. B.: Anatomy of a diffuse cryptic suture zone: An example from the Bohemian Massif, European Variscides, Geology, 42, 275–278, https://doi.org/10.1130/G35290.1, 2014.

Seghedi, I. and Downes, H.: Geochemistry and tectonic development of Cenozoic magmatism in the Carpathian–Pannonian region, Gondwana Research, 20, 655–672, https://doi.org/10.1016/j.gr.2011.06.009, 2011.

Seghedi, I., Ersoy, Y. E., and Helvacı, C.: Miocene–Quaternary volcanism and geodynamic evolution in the Pannonian Basin and the Menderes Massif: A comparative study, Lithos, 180, 25–42, doi.org/10.1016/j.lithos.2013.08.017, 2013.

Serpelloni, E., Vannucci, G., Anderlini, L., and Bennett, R. A.: Kinematics, seismotectonics and seismic potential of the eastern sector of the European Alps from GPS and seismic deformation data, Tectonophysics, 688, 157–181, doi.org/10.1016/j.tecto.2016.09.026, 2016.

Serretti, P. and Morelli, A.: Seismic rays and traveltime tomography of strongly heterogeneous mantle structure: application to the Central Mediterranean, Geophys. J. Int., 187, 1708–1724, https://doi.org/10.1111/j.1365-246X.2011.05242.x, 2011.

Shito, A., Karato, S., Matsukage, K., N., and Nishihara Y.: Towards Mapping the Three-Dimensional Distribution of Water in the Upper Mantle from Velocity and Attenuation Tomography, Geophysical Monograph, 168, 225–236, https://doi.org/10.1029/168GM17, 2006.

Singer, J., Diehl, T., Husen, S., Kissling, E., and Duretz, T.: Alpine lithosphere slab rollback causing lower crustal seismicity in northern foreland, Earth Planet. Sc. Lett., 397, 42–56, doi.org/10.1016/j.epsl.2014.04.002, 2014.

Smye, A. J., Bickle, M. J., Holland, T. J. B., Parrish, R. R., and Condon, D. J.: Rapid formation and exhumation of the youngest Alpine eclogites: A thermal conundrum to Barrovian metamorphism, Earth Planet. Sc. Lett., 306, 193–204, https://doi.org/10.1016/j.epsl.2011.03.037, 2011.

Spada, M., Bianchi, I., Kissling, E., Piana Agostinetti, N., and Wiemer, S.: Combining controlled-source seismology and receiver function information to derive 3-D Moho topography for Italy, Geophys. J. Int., 194, 1050–1068, https://doi.org/10.1093/gji/ggt148, 2013.

Spakman, W. and Wortel, M. J. R.: Tomographic View on Western Mediterranean Geodynamics, in: The TRANSMED Atlas, The Mediterranean Region from Crust to Mantle, edited by: Cavazza, W., Roure, F. M., Stampfli, G. M., and Ziegler, P. A., Springer, Berlin, Heidelberg, 31–52, https://doi.org/10.1007/978-3-642-18919-7_2, 2004.

Speranza, F., Villa, I. M., Sagnotti, L., Florindo, F., Cosentino, D., Cipollari, P., and Mattei, M.: Age of the Corsica–Sardinia rotation and Liguro–Provençal Basin spreading: new paleomagnetic and Ar/Ar evidence, Tectonophysics, 231–251, https://doi.org/10.1016/S0040-1951(02)00031-8, 2002.

Stipčević, J., Tkalčić, H., Herak, M., Markušić, S., and Herak, D.: Crustal and uppermost mantle structure beneath the External Dinarides, Croatia, determined from teleseismic receiver functions, Geophys. J. Int., 185, 1103–1119. https://doi.org/10.1111/j.1365-246x.2011.05004.x, 2011.

Stipčević, J., Herak, M., Molinari, I., Dasović, I., Tkalčić, H., and Gosar, A.: Crustal thickness beneath the Dinarides and surrounding areas from receiver functions, Tectonics, 37, https://doi.org/10.1029/2019TC005872, 2020.

Sun, W., Zhao, L., Malusà, M. G., Guillot, S., and Fu, L.-Y.: 3-D Pn tomography reveals continental subduction at the boundaries of the Adriatic microplate in the absence of a precursor oceanic slab, Earth Planet. Sc. Lett., 510, 131–141, 2019. https://doi.org/10.1016/j.epsl.2019.01.012

Tesauro, M., Kaban, M. K., and Cloetingh, S. A. P. L.: EuCRUST-07: A new reference model for the European crust, Geophys. Res. Lett., 35, L05313, https://doi.org/10.1029/2007/g032244, 2008.

Ustaszewski, K., Schmid, S. M., Fügenschuh, B., Tischler, M., Kissling, E., and Spakman, W.: A map-view restoration of the Alpine–Carpathian–Dinaridic system for the Early Miocene, Swiss J. Geosci., 101, 273–294, https://doi.org/10.1007/s00015-008-1288-7, 2008.

Verwater, V. F., Le Breton, E., Handy, M. R., Picotti, V., Jozi Najafabadi, A., and Haberland, C.: Neogene kinematics of the Giudicarie Belt and eastern Southern Alpine orogenic front (northern Italy), Solid Earth, 12, 1309–1334, https://doi.org/10.5194/se-12-1309-2021, 2021.

van der Meer, D. G., Spakman, W., van Hinsbergen, D. J. J., Amaru, M. L., and Torsvik, T. H.: Towards absolute plate motions constrained by lower-mantle slab remnants, Nat. Geosci., 3, 36–40, 2010.

van der Meer, D. G., van Hinsbergen, D. J. J., and Spakman, W.: Atlas of the underworld: Slab remnants in the mantle, their sinking history, and a new outlook on lower mantle viscosity, Tectonophysics, 723, 309–448, doi.org/10.1016/j.tecto.2017.10.004, 2018.

van Hinsbergen, D. J. J., Torsvik, T. H., Schmid, S. M, Matenco, L. C., Maffione, M., Vissers, R. L .M., Gürer, D., and Spakman, W.: Orogenic architecture of the Mediterranean region and kinematic reconstruction of its tectonic evolution since the Triassic, Gondwana Research, 81, 79–229, https://doi.org/10.1016/j.gr.2019.07.009, 2020.

von Blanckenburg, F. and Davies, J. H.: Slab breakoff: A model for syncollisional magmatism and tectonics in the Alps, Tectonics, 14, 120=-131, doi.org/10.1029/94TC0205, 1995.

Waldhauser, F., Lippitsch, R., Kissling, E., and Ansorge. J.: High-resolution teleseismic tomography of upper-mantle structure using an a priori three-dimensional crustal model, Geophys. J. Int., 150, 403–414, doi.org/10-1046/j.1365-246X.2002.01690.x, 2002.

Wortel, M. J. R. and Spakman, W.: Subduction and Slab Detachment in the Mediterranean-Carpathian Region, Science, 290, 1910–1917, https://doi.org/10.1126/science.290.5498.1910, 2000.

Zahorec, P., Papčo, J., Pašteka, R., Bielik, M., Bonvalot, S., Braitenberg, C., Ebbing, J., Gabriel, G., Gosar, A., Grand, A., Götze, H.-J., Hetényi, G., Holzrichter, N., Kissling, E., Marti, U., Meurers, B., Mrlina, J., Nogová, E., Pastorutti, A., Salaun, C., Scarponi, M., Sebera, J., Seoane, L., Skiba, P., Szűcs, E., and Varga, M.: The first pan-Alpine surface-gravity database, a modern compilation that crosses frontiers, Earth Syst. Sci. Data, 13, 2165–2209, https://doi.org/10.5194/essd-13-2165-2021, 2021.

Zhao, L., Paul, A., Guillot, S., Solarino, S., Malusá, M., Zheng, T., Aubert, C., Dumont, T., Schwartz, S., Zhu, R., and Wang, Q.: First seismic evidence for continental subduction beneath the Western Alps, Geology, 43, 815–818, https://doi.org/10.1130/G36833.1, 2015.

Zhao, L., Paul, A., Guillot, S., Solarino, S., Malusà, M.G., Zheng, T., Aubert, C., Salimbeni, S., Dumont, T., Schwartz, S., Zhu, R. and Wang, Q.: Continuity of the Alpine slab unraveled by high-resolution P wave tomography, J. Geophys. Res., Solid Earth, 121, 8720–8737, https://doi.org/10.1002/2016jb013310, 2016.

Remarks from the language copy-editor

CE1   This is the standard English-language spelling of the city (see https://www.lexico.com/definition/zurich).

Remarks from the typesetter

TS1   The companion paper will be updated by us.